筑　波　大　学

University of Tsukuba

博　士　（人間生物学）　学　位　論　文

PhD dissertation in Human Biology

筑　波　大　学

University of Tsukuba

博　士　（人間生物学）　学　位　論　文

PhD dissertation in Human Biology

Generation of new genetically modified mice for phenotyping of oocytes with impaired FOXO3 nuclear export

(新規遺伝子改変マウスを用いた卵母細胞の生存における核内 FOXO3 の機能解析)

2021

筑波大学グローバル教育院

School of the Integrative and Global Majors in University of Tsukuba

Ph.D. Program in Human Biology

HOAI THU LE

LIST OF ABBREVIATIONS

CA	Constitutively active
cKI	Conditional knock-in
cKO	Conditional knock-out
E18.5	Embryonic day 18.5
GC	Granulosa cell
H and E	Hematoxylin and Eosin
IVF	*In vitro* fertilization
MT-NES	Mutated nuclear export sequence
NES	Nuclear export sequence
POI	Premature ovarian insufficiency
PD1	Postnatal day 1
PD3	Postnatal day 3
PD6	Postnatal day 6
PD45	Postnatal day 45
PCR	Polymerase chain reaction
TAM	Tamoxifen
WT-NES	Wildtype nuclear export sequence
WT	Wildtype

TABLE OF CONTENTS

ABSTRACT

Germ cell development is a fundamental process for maintaining reproduction in animals. In mammalian females, the ovarian reserve is vital for determining the length of the fertility life span. PI3K/Akt is a well-known signaling pathway that controls the maintenance and activation of dormant primordial oocytes. The nucleus-to-cytoplasm translocation and the loss of FOXO3, a member of the PI3K/Akt pathway, causes the activation of these dormant oocytes. However, it is not clear whether the accumulation of FOXO3 in the oocyte nucleus causes oocyte death or prolongs its survival. To examine the exact outcome of abnormal accumulation of nuclear FOXO3, I developed a novel *Foxo3* constitutively active (CA) conditional knock-in (cKI) mice. The mouse line carries mutations in the nuclear export sequence (NES), which can prevent FOXO3 translocation. To investigate the role of nuclear FOXO3 in ovarian reserve before and after sex maturation, I developed three novel bioresources and established two mouse models (congenital and acquired). The results presented in this work revealed that the accumulation of nuclear FOXO3 caused a significant increase in the number of primordial oocytes in both the models. This indicates that the accumulation of FOXO3 in the oocyte nucleus can promote the extended survival of dormant primordial oocytes.

INTRODUCTION

In mammals, particularly females, ovarian reserve is important, as it indicates female fertility. Oogenesis is a critical developmental process in which fertilizable oocytes are produced from oogonia in the ovaries. During embryogenesis, oogonia are formed and differentiate into oocytes that are enclosed in primordial follicles [1]. The initial pool consists of a certain number of primordial follicles that are maintained in the dormant stage of the ovary. The population of these primordial follicles gradually declines with age [2, 3, 4]. During puberty, a small proportion of primordial follicles is activated, recruited into the growing pool, and develops into primary follicles through the primordial follicle activation process [5]. Some primary follicles continue to grow until ovulation, whereas others undergo apoptosis (Figure 1). The remaining follicles are either maintained in the ovary or lost with age. Most primordial follicles remain dormant for a long period within the female's fertility life span. In humans, follicles can be preserved for 50 years, and in mice these can be preserved for more than one year. The dormancy and activation of the above-described primordial follicle process is important for determining the length of fertility period duration because the follicle population cannot be expanded or renewed, and they serve as the only potential source for reproduction [6, 7]. The exhaustion of the primordial follicle pool can lead to depletion of the ovarian reserve. Abnormal or excessive activation can cause ovarian diseases such as premature ovarian insufficiency (POI) [8, 9, 10, 11]. Such disorders can lead to improper oogenesis and subsequent infertility in women.

Several studies have attempted to identify the mechanisms controlling primordial follicle reserve and activation [12, 13, 14]. However, the extent to which these dormant follicles are selectively recruited for growth is unknown. The

phosphoinositide 3 kinase (PI3K)-Akt pathway is known to play a major role in primordial follicle activation [15]. This intercellular signaling pathway is involved in various cellular processes. Activation of this pathway results in the phosphorylation of its downstream target FOXO3 and subsequent FOXO3 translocation from the nucleus to the cytoplasm [16]. FOXO3, a transcriptional factor, belongs to the FOXO family, which includes FOXO1, FOXO3, FOXO4, and FOXO6. FOXO3 is involved in various fundamental cellular processes, such as proliferation, differentiation, apoptosis, and stress resistance [17]. During oogenesis, it acts as a key regulator of primordial follicle activation in a PI3K-Akt dependent manner. In particular, FOXO3 is actively located in the nucleus, where it functions as a transcriptional factor to initiate the transcription of its target genes that are required for cell cycle arrest or apoptosis [18, 19]. Under PI3K/Akt pathway activation, FOXO3 is phosphorylated at threonine 32, serine 253, and 315 by Akt and is exported to the cytoplasm, thereby promoting cell proliferation (Figure 2). The deletion of *Foxo3* does not cause embryonic lethality in mice; however, it induces global primordial follicle activation and subsequent follicle depletion, leading to sterility in 15-week-old females [20].

Although the function of FOXO3 translocation in oogenesis has been clearly described, the effects of high FOXO3 accumulation in the oocyte nucleus on the maintenance of oocyte dormancy have been reported contentiously. In a previous study, the accumulation of nuclear FOXO3 in oocytes from oocyte-specific receptor tyrosine kinase (*Kit*) conditional knockout (cKO) mice led to the complete failure of oocyte reawakening in dormant follicles; eventually, all oocytes from cKO mice underwent apoptosis at 6 months of age [21]. In contrast, another study reported that mutant oocytes carrying *Foxo3* mutation in the phosphorylation sites, therefore constitutively

active FOXO3 in the nucleus, could enhance fertility in aged females; thus, this mutation was found to prolong the maintenance of primordial follicles [22]. These two studies reported conflicting results regarding the effect of the accumulation of nuclear FOXO3 on the maintenance of dormant follicles. However, the above-mentioned mouse models exhibit some limitations. It is difficult to precisely assess the role of nuclear FOXO3 in oocyte development. In detail, the transgenic mice expressed a FOXO3 protein mutated at the following phosphorylation sites: threonine 32, serine 253, 315, 318, 321, and 325, under the *c-Kit* promoter [22]. These mutations may disturb positive functional interactions between FOXO3 and other proteins or between FOXO3 and the corresponding DNA binding sequence, thereby inhibiting its role as a regulator of primordial follicle activation. In addition, the expression of the transgene was controlled by the *c-Kit* promoter, which may differ from the endogenous expression of *Foxo3*. In the other mouse model used in previous studies, when *c-Kit* was deleted, the PI3K/Akt pathway regulating FOXO3 export was consequently interrupted [21]. Since *c-Kit* is upstream signaling in oocytes, not only FOXO3 export was disrupted but also other possible downstream pathways may have been muddled. These pathways may be involved in regulating oocyte development, such as controlling dormant oocyte survival. Such distortion in those pathways may lead to the observed phenotype, confusing the actual contribution of oocyte nuclear FOXO3 accumulation to the maintenance of dormant oocytes. Moreover, the consequence of high FOXO3 nuclear accumulation in the oocyte has not been deeply investigated. To examine the exact outcome of the high accumulation of nuclear FOXO3, I developed a novel *Foxo3* constitutively active (CA) conditional knock-in (cKI) mice using the Cre-loxP system. This mutated *Foxo3* harbors a mutation in the NES

sequence that can prevent nuclear-to-cytoplasmic FOXO3 translocation. This mutation resulted in a high accumulation of FOXO3 in the nucleus of primary oocytes. The initial primordial oocyte pool in newborn mice was found to be maintained at the dormant stage, although a part of this cohort was depleted between postnatal day 6 (PD6) and 45 (PD45) [23]. It is still unclear how the primordial oocytes in the initial pool are fated to death or survival, and what criteria decide this selection before sex maturation. When the mice reached sexual maturation, the loss of primordial oocytes was much more modest [23]. It is difficult to determine the fate of oocytes through depletion after sex maturation. Thus, the concept of primordial oocyte reserves before and after sex maturation has not been elucidated [24]. Particularly, the question of whether the accumulation of nuclear FOXO3 affects oocyte reserve differently before and after sex maturation needs to be investigated. Therefore, to address this question, I used two models, congenital and acquired, to reveal how profoundly the nuclear FOXO3 levels affected the maintenance and activation of the oocyte pool. In this study, I created two novel Cre driver mice, *Gdf9*^{Cre} and *Ddx4*^{CreERT2}, to induce Cre recombination in *Foxo3*-CA cKI mice. To establish the congenital model, a *Gdf9*^{Cre} mouse strain, with recombination occurring from PD3, was used. Thus, in this model, FOXO3 accumulated in the oocyte nucleus from PD3, helping to investigate the impact of nuclear FOXO3 accumulation on oocyte reserve before sex maturation. In contrast, *Ddx4*^{CreERT2} mice with Cre recombinase activity controlled by tamoxifen (TAM) injection were utilized to establish the acquired model. In this model, TAM administration was performed at the age of 8-weeks, causing FOXO3 accumulation in the oocyte nucleus after the mice were sexually mature. This acquired model was used

to determine whether nuclear FOXO3 influenced the maintenance of primordial oocytes after sex maturation and before aging.

According to the results gathered herein, FOXO3 was highly accumulated in the nucleus of primary oocytes from cKI mice in both congenital and acquired models. This result proved that the mutation in NES successfully prevented FOXO3 from exporting to the oocyte cytoplasm. Gathering the results obtained for the characterization of the oocyte reserve, a significant increase in the number of dormant primordial oocytes in both models of cKI mice was observed. These results indicate that the accumulation of FOXO3 in the oocyte nucleus can prolong the survival of dormant primordial oocytes.

METHODS

1. Mice and Animal Experiment Ethics

All animal experiments were carried out in a humane manner, with approval from the Institutional Animal Experiment Committee of the University of Tsukuba following the Regulations for Animal Experiments of the University of Tsukuba and the Fundamental Guidelines for Proper Conduct of Animal Experiments and Related Activities in Academic Research Institutions under the jurisdiction of the Ministry of Education, Culture, Sports, Science, and Technology of Japan. All mice used in this study were kept in specific pathogen-free conditions at the Laboratory Animal Resource Center at the University of Tsukuba. *R26GRR* mice were used to investigate Cre recombination in all the tissues [25].

2. Vector and microinjection

The *pX330* vector for Cas9 and sgRNA were used to generate three knock-in mouse lines [44]. The knock-in donor plasmids consisted of a CRISPR target and knock-in sequence. Each *pX330* vector (5 ng/μl) and each knock-in donor plasmid (10 ng/μl) were mixed and filtered using a 0.22 mm PVDF syringe filter (MILLEX-GV®, Merck-Millipore). For microinjection, C57BL/6J female mice were stimulated to super-ovulate by injection of pregnant mare serum gonadotropin (5 units) (ASKA Pharmaceutical Co. Ltd.) and human chorionic gonadotropin (5 units) (ASKA Pharmaceutical) with a 48-hour interval and naturally mated with C57BL/6J male mice to collect embryos. The vectors were co-microinjected into male pronuclei of the collected zygotes. Subsequently, the living embryos were transferred into the oviducts of pseudo-pregnant ICR female mice. The desired mice were selected for PCR analysis.

3. Genotyping

Genomic DNA was extracted from the tail tips of 3-week-old mice, using lysis buffer (1 M Tris-HCl/ 5 M NaCl/ 0.5 M EDTA, 10% SDS) and Proteinase K (10%), and purified with phenol-chloroform. The purified genomic DNA was lysed in 40 µL TE buffer (10 mM TRIZMA BASE/ 1 mM EDTA/ H_2O) (pH 8.0). PCR was carried out with PrimeSTAR GXL DNA Polymerase (Takara) or AmpliTaq Gold 360 Master Mix (Thermo Fisher Scientific) using the primers listed in Table 1.

4. Electroporation

Cre mRNA was introduced into zygotes via electroporation refer previous paper [45]. The electroporated embryos were then transferred into pseudopregnant mice. The pups were obtained at PD1.

5. Tissue collection and embedment

Mice were anesthetized with a 10% pentobarbital/saline solution and subjected to heart perfusion with a PBS solution. After, the testes or ovaries were collected. For frozen sections, the tissues were immersed in 4% paraformaldehyde at 4°C overnight, followed by equilibration in gradually increasing concentrations of sucrose/PBS solutions (10%, 20%, and 30%). They were then placed in Tissue-Tek® OCT Compound and kept frozen at -80°C. For paraffin sections, the ovaries were submerged in 10 NM Mildform (Fuji Film Wako Pure Chemical Industries, Ltd.) at 4°C overnight. They were then soaked in 70% ethanol overnight and embedded in paraffin. The frozen and paraffin sections were dissected with a thickness of 5 µm. Paraffin sections were sliced and dried at 37°C overnight.

6. Hematoxylin and eosin (H and E) staining

The 5 µm paraffin sections were deparaffinized and refixed with 10 NM Mildform for 30 min. They were then submerged in Meyer hematoxylin solution (Fujifilm Wako Pure Chemical Industries, Ltd.) at room temperature for 15 min. Subsequently, they were washed with running tap water. They were stained with 1% Eosin Y solution (Fujifilm Wako Pure Chemical Industries, Ltd.) at room temperature for 5 min. Next, the slides were dehydrated and permeated with ethanol and xylene. Finally, they were mounted with EUKITT® mounting medium for analysis. The H-and E-stained specimens were observed using an all-in-one fluorescence microscope BZ-X710 (KEYENCE).

7. Immunofluorescence staining

The frozen sections were dried at room temperature and washed twice with PBS for 10 min. They were then incubated in 0.25% Triton X-100/ PBS solution at room temperature for 30 min, followed by membrane permeation treatment. The slides were then washed twice with PBS for 10 min and blocked with blocking buffer (10% goat serum/ 0.01% tween-20/ 0.1% BSA/ PBS) for 60 min at room temperature. The slides were then incubated with primary antibody solution. Depending on the primary antibodies, the sections were incubated at 4°C overnight or at room temperature for 60 min. After washing twice with PBS for 10 min, the sections were incubated with the appropriate secondary antibody solution at room temperature for 60 min while blocking the light. They were then washed twice with PBS for 10 min. In some experiments, the testes sections were stained with Alexa Fluor 647 conjugated PNA-lectin (Thermo Fisher Scientific, 1:100) for 1 h at room temperature. After secondary antibody incubation, the sections were washed with PBS for 10 min and stained with 4', 6-diamidino-2-phenylindole (DAPI) for 5 min at room temperature. The sections

were washed with PBS for 5 min and mounted with a prolonged gold antifade reagent with DAPI (Thermo Fisher Scientific).

For paraffin sections, the slides were deparaffinized, and membrane permeation was performed using 0.25% TritonX-100/ PBS solution at room temperature for 20 min. After washing twice with PBS for 10 min, antigen retrieval was performed by autoclaving at 121°C for 10 minutes in the Target Retrieval Solution (DAKO) solution. After that, the sections were washed twice with PBS for 10 min and blocked with blocking solution. The slides were then incubated with the primary antibody at 4°C overnight. The slides were then washed twice with PBS for 10 min. The antigen was visualized by incubation with an appropriate secondary antibody. In some experiments, after secondary antibody staining, the sections were stained with wheat germ agglutinin (WGA) CF® 488A conjugates (Biotium) for 15 min at room temperature. The sections were then followed by nuclear staining and mounting using the same procedure as for frozen sections. The specimens were observed using an all-in-one fluorescence microscope BZ-X710 (KEYENCE) or a confocal microscope Leica SP8 (Leica Microsystems). All antibodies used for immunofluorescence staining are shown in Table 2.

8. RT-qPCR

The testes and thymus from *Ddx4*^{CreERT2} mice were collected and homogenized. Total RNA was isolated using the NucleoSpin RNA kit (Macherey-Nagel). cDNA was synthesized using dT PrimeScript™ RT Master Mix (Perfect Real Time) (Takara), and RT-PCR for Ddx4 was performed. Relative gene expression was normalized to that of *GAPDH*. Quantitative PCR was carried out using a Thermal Cycler Dice Real Time

System (Takara) with Thunderbird™ SYBR® qPCR mix. *Actb* was used as a housekeeping gene for normalizing the relative gene expression. The primers used for RT-qPCR are shown in Table 3.

9. Tamoxifen (TAM) injection

Mice were injected with TAM to induce Cre recombination. TAM (Sigma-Aldrich) was dissolved in corn oil at a concentration of 20 mg/ml and shaken overnight at 37°C. Each adult mouse received a dosage of 0.1 mg/g of body weight by intraperitoneal injection. The mice were injected with TAM consecutively for 4 days, followed by 3-days' rest, 4-days' injection, and 1-week rest periods.

10. *In vitro* fertilization (IVF) and *in vitro* culture of embryos

IVF was performed using sperm and oocytes to confirm that all sperm were completely recombined. Fertilized eggs were cultured in an incubator at 37°C, 5% CO_2. The embryos were analyzed at embryonic day 3.5 (E3.5). Fertilized zygotes from IVF were transplanted into pseudo-pregnant mice and analyzed at embryonic day 18.5 (E18.5) for EGFP and tDsRed fluorescence using a stereomicroscope.

11. Oocyte counting by H and E staining

HE-stained 5 μm-thick continuous section specimens were prepared. Next, four consecutive sections and a total of 12 sections were dissected to obtain the largest number of oocytes for measurement. Oocytes that had clear nuclei were chosen for counting. To discriminate the developmental stage, morphological changes in the granulosa cells surrounding the oocytes were examined.

12. Image analysis of fluorescence signal

FOXO3 and MVH were co-immunostained using 5 μm ovary paraffin sections. The slides were analyzed using a confocal microscope Leica SP8 (Leica Microsystems). In total, 30 primary oocytes from each group were randomly selected for quantification. First, the cytoplasmic region of oocytes was identified using the MVH signal. The nuclear area of oocytes was distinguished by DAPI staining. The intensity brightness of the FOXO3 signal in the oocyte nucleus was measured. In addition, the nuclear FOXO3 signal was subtracted from the image and the brightness was measured as the FOXO3 signal in the cytoplasm. All image analyses were performed using ImageJ software.

13. Oocyte diameter measurement

The paraffin-embedded ovary was sliced to a thickness of 5 μm and co-stained with MVH, PCNA, and WGA. The follicle region was detected by the WGA signal as it labeled the cell membrane. Oocytes with a single layer of granulosa cells (GCs) were measured, and the total number of oocytes of each genotype was counted in a total of 12 sections. Then, using images in which nucleoli were observed in these oocytes, the diameter was measured using ImageJ.

14. Western blotting

Testes were homogenized in T-PER Tissue Protein Extraction Reagent (Thermo Fisher Scientific). Each protein (37.5 mg) was resolved by 7.5% sodium dodecyl sulfate-polyacrylamide gel electrophoresis (SDS-PAGE) gel electrophoresis and transferred to Immobilon-P PVDF membrane (Merck-Millipore). The membrane was blocked with 5% skim milk in Tris-TBS buffer for 30 min. The membrane was subsequently incubated

with the primary antibody solution for 4 h at room temperature. The anti-mouse GAPDH antibody was used as an internal control. The membrane was then incubated with a secondary antibody solution for 30 min at room temperature. The blots were developed by chemiluminescence using ImmunoStar LD's protocol (Wako) and visualized using iBrightCL100 (Thermo Fisher Scientific). The antibodies used in this experiment are summarized in Table 2.

15. Statistical analysis

The number of follicles, the ratio of cytoplasmic and nuclear FOXO3, and the diameter of primary follicles were tested for statistical significance. Prism was used to perform unpaired Student's t-tests and graph productions. Differences were considered significant at $p<0.05$.

RESULTS

1. Development of mouse resources

1.1 Production of novel mouse lines

1.1.1 *Gdf9^{Cre}* Cre driver mice production

To establish the congenital model, germ cell-specific *Gdf9^{Cre}* mice were created. Growth and differentiation 9 (GDF9) is an oocyte-secreting factor that promotes oocyte development and granulosa cell growth, as it is needed for the growth of primary follicles. *Gdf9* transcripts are also found in murine female germ cells from embryonic day 19.5 (E19.5) [26, 27]. Since *Gdf9* is expressed in oocytes, the promoter of this gene was used for Cre expression in oocytes. Previously, transgenic Tg(Gdf9-icre)5092Coo/J mice express transgenes with unknown insertion sites and unfamiliar genetic backgrounds [28]. These features may result in recombination at undesired tissues. For these reasons, I generated *Gdf9^{Cre}* knock-in mice by CRISPR/Cas9. The P2A connected with the NLS-Cre-pA sequence was knocked-in immediately just before the *Gdf9* stop codon (Figure 3). This construction has great advantages over the random insertion technique used in the previous mouse line. Moreover, the genetic background of Cre driver mice is C57BL6/J, which is common in genetically modified mouse models. Taken together, I produced a novel *Gdf9^{Cre}* Cre driver mice, which is applicable in female germ cell research.

1.1.2 *Ddx4^{CreERT2}* Cre driver production

To obtain the acquired model, I developed a novel bicistronic *Ddx4^{CreERT2}* knock-in driver mouse strain. DDX4 is an ATP-dependent RNA helicase that is highly conserved

in the germ cell lineages of various species. It is expressed in both male and female murine germ cells. Particularly, in females, DDX4 starts to be expressed in the cytoplasm of primordial oocytes and gradually decreases as maturation proceeds until it finally disappears in mature oocytes. In males, DDX4 is detected in germ cells from spermatogonia to round spermatids [29]. Since *Ddx4* is specifically expressed in germ cells, its promoter has been widely used for germ cell-specific CreERT2 expression. In the *Ddx4*^{CreERT2} mice, the 2A sequence-connected *CreERT2* gene was knocked in just before the *Ddx4* stop codon (Figure 4A). Thus, this construction prevented disruption of the *Ddx4* gene itself. The knocked-in allele and random integration were confirmed by polymerase chain reaction (PCR) (Figure 4B).

1.1.3 Foxo3-CA cKI production

In previous studies, two different mouse models that possessed nuclear FOXO3 accumulation in oocytes were reported to have two controversial phenotypes in oocyte reserve. The conflict in these phenotypes may be due to the disadvantages of the mouse models used. In the first model, the mutation of *Foxo3* at threonine 32 and serine 253, 315, 318, 321, and 325, which are FOXO3 phosphorylation sites, promoted oocyte survival as the number of follicles at all stages was reported to be increased [22]. However, this mutation may interrupt the interactions between FOXO3 and other factors, such as protein or DNA binding. On the other hand, *c-Kit* conditional knockout mice (cKO) exhibited oocyte death. This phenotype can result from the disruption of not only the PI3K/Akt pathway but also other positive downstream signaling pathways of c-KIT, which may be the actual cause of oocyte death [21].

To overcome the weakness of the previous mouse models [21, 22], I established a novel *Foxo3* constitutively active (CA) cKI mice that express *Foxo3* with a mutated nuclear export sequence (NES), in a Cre-dependent manner. NES is important for the transportation of components from the nucleus to the cytoplasm. It was reported that the mutation in this sequence does not affect the normal function and structural conformation of FOXO3 in the nucleus [30]. Thus, in this study, a mutated NES containing the substitution of seven critical amino acids for alanine was generated (Figure 5A). The NES mutation only inhibits the nuclear export of FOXO3 without affecting the phosphorylation sites and positive functional interactions between FOXO3 and other factors. This strategy conquers the limitations and weaknesses of the previous gene-modified animal model, as well as the benefit of studying the interaction of FOXO3 with other targets involved in primordial follicle maintenance and activation.

To avoid embryonic lethality, conditional knock-in (cKI) mice using the constitutively active (CA) FLEX allele was created [31, 32, 33]. In the FLEX system, the direction of the gene expression before and after Cre recombination was inverted. Thus, in principle, there is no leakage of the latter gene expression. This system requires at least two different Lox sequences. In this study, LoxP and Lox2272 were used. In the CA FLEX allele, the second exon of *Foxo3* containing the NES without mutation (WT-NES) was in the forward orientation and the one carrying the NES with the mutation (MT-NES) was in reverse orientation (Figure 5B). The knocked-in allele was confirmed by polymerase chain reaction (PCR) (Figure 5C, D).

1.2 Evaluation the quality of bioresources

1.2.1 *Gdf9^{Cre}* mouse evaluation

To check whether the *Gdf9^{Cre}* mice were suitable for germ cell research, the mouse phenotype and Cre recombination activity were examined. The heterozygous *Gdf9$^{Cre/+}$* mice showed normal ovarian morphology and a comparable number of oocytes at all stages compared with wild-type mice (Figure 6A, B). Notably, the homozygous *Gdf9$^{Cre/Cre}$* ovaries showed a significant increase in the diameter of the primary oocytes (Figure 6A, C). Moreover, no secondary or further developmental stages of follicles were detected in homozygous females, indicating that primary oocytes from homozygous *Gdf9$^{Cre/Cre}$* mice failed to proceed to further follicle developmental stages. It is known to GDF9 regulates granulosa cell proliferation [46, 47]. The disruption of GDF9 can cause folliculogenesis arrest beyond the primary stage and may eventually increase oocyte size. This result indicated that the function of GDF9 was interrupted in homozygous *Gdf9$^{Cre/Cre}$* mice, leading to the failure of granulosa cell differentiation, while the oocytes could grow and increase their diameter.

Next, to examine Cre recombinase activity in *Gdf9^{Cre}* mice, *Gdf9^{Cre}* mice were mated with the reporter R26GRR mice (*ROSA^{GRR}*), which expresses EGFP and tDsRed before and after Cre recombination, respectively [25]. Four litters obtained from *Gdf9$^{+/Cre}$*::*ROSA$^{GRR/GRR}$* (♀) and WT (♂) mating consisted of tDsRed-positive and no fluorescence offspring. No GFP-positive pups were found among the litters (Figure 6D). This means that oocytes from *Gdf9$^{Cre/+}$* females recombined completely. In contrast, the offspring of six litters obtained from *Gdf9$^{+/Cre}$*::*ROSA$^{GRR/GRR}$* (♂) and WT (♀) showed only GFP-positive and no fluorescence signals, indicating that Cre recombination only occurred in female, but not male germ cells (Figure 6E).

The stages of oocyte development in which Cre recombination occurred were examined. It was shown that recombination began with primordial oocytes in the ovary (Figure 7A, B, C). At birth (PD0), no tDsRed-positive oocytes were observed, indicating that Cre recombination had not yet begun. Until PD3, tDsRed-positive oocytes appeared, although some oocytes were still GFP positive (Figure 7D). This result confirmed that Cre recombinase activity in *Gdf9*^{Cre} mice occurred from PD3, and the oocytes were completely recombined in adult mice. To confirm that recombination only occurred in female germ cells but not in other unspecific tissues, tDsRed signal in various tissues of *Gdf9*^{Cre} mice, including the testis, was examined. There was no tDsRed signal observed in other tissues, except in the cerebellum and testis (Figure 7E, F, G). Taken together, *Gdf9*^{Cre} mice are a beneficial tool for studying female germ cell development.

1.2.2 *Ddx4*^{CreERT2} mouse evaluation

To evaluate the quality of *Ddx4*^{CreERT2}, I first checked whether germ cell development appeared abnormally in knock-in mice before Cre recombination. The homozygous *Ddx4*^{CreERT2} females appeared to have oogenesis similar to that of wild-type mice (Figure 8A). In contrast, sperms from heterozygous knock-in males were observed to have elongated nuclei. Surprisingly, there was no sperm in the homozygous knock-in males. The marker for the acrosome, peanut agglutinin (PNA)-lectin, was found in round spermatids, which had a small spherical nucleus in homozygous knock-in males (Figure 8A). This result indicated that spermatogenesis stopped at the round spermatid phase in the homozygous but not stopped in the heterozygous. *Ddx4* mRNA expression was observed to decrease in homozygous knock-in testes (Figure 8B). Next,

the DDX4 protein level and ribosomal skipping between *Ddx4* and *CreERT2* were confirmed by western blotting. The protein level of DDX4 decreased in homozygote testes, which was consistent with the RT-qPCR results (Figure 8D, E). The expected size of simple DDX4, but not the DDX4-CreERT2 fusion protein, was detected (Figure 8C). This result suggested the possibility that reduced *Ddx4* expression prevented the differentiation of round spermatids into mature sperms.

To investigate Cre recombinase activity in $Ddx4^{CreERT2}$ mice, $Ddx4^{CreERT2}$ mice were mated with the reporter R26GRR mice ($ROSA^{GRR}$). $Ddx4^{CreERT2}$::$ROSA^{GRR}$ mice underwent TAM administration at 8-weeks old. The fluorescence signals were then observed in TAM-treated or non-treated $Ddx4^{CreERT2}$::$ROSA^{GRR}$ mice at 11-weeks old. As expected, tDsRed signals were observed in the ovaries and testes of $Ddx4^{CreERT2}$::$ROSA^{GRR}$ males (Figure 9A). To further confirm whether unspecific Cre recombination occurred in other tissues, tDsRed signals were examined in various organs. As expected, there was no tDsRed signal in the TAM-non-treated mice. In contrast, there was no tDsRed signal in non-reproductive tissues, except for the thymus and pancreas in TAM-treated $Ddx4^{CreERT2}$::$ROSA^{GRR}$ mice (Figure 9B). EGFP and tDsRed signal were detected in these two tissues (Figure 10A). Moreover, *Ddx4* expression in thymus was confirmed by RT-PCR (Figure 10B). The expression of this gene was also detected in the mouse pancreas using Fantom5 (http://fantom.gsc.riken.jp/5/sstar/Main_Page). Taken together, these results indicate that Cre recombination mainly occurs in the ovaries and testes. Weak fluorescent protein occurred in a part of the thymus and pancreas via *Ddx4* endogenous promoter activities.

The competence of Cre recombination in female germ cells was then checked using anti-DDX4 antibody, a germline cytoplasmic marker in immature oocytes. All DDX4-positive 44 oocytes expressed the tDsRed signal (Figure 11), whereas there was no recombined signal detected in somatic cells, such as granulosa or theca cells. This confirmed that recombination occurred in all oocytes during oogenesis, but not in somatic cells in the ovary.

In the TAM-treated *Ddx4*^{CreERT2}*::ROSA*^{GRR} testes, only tDsRed was detected at the center of the seminiferous tubules (Figure 12A). To evaluate the efficiency of Cre recombination, IVF using sperm from TAM-treated *Ddx4*$^{CreERT2/+}$::*ROSA*$^{GRR/+}$ mice and unfertilized wild-type oocytes was performed. Fertilized zygotes were allowed to develop into blastocysts via *in vitro* culture until embryonic day 18.5 (E18.5). Half (22/45) of the blastocysts displayed tDsRed (Figure 12B). Some embryos stopped developing prior to the morula stage. No EGFP signal was detected in any blastocyst. Similar results were obtained in embryos at E18.5. In addition, tDsRed signals were observed in 29/60 E18.5 embryos and no EGFP-positive embryos (Figure 12C). According to the above results, *Ddx4*^{CreERT2} was able to induce Cre recombination with 100% efficiency in male germ cells.

To examine whether Cre recombination occurred in undifferentiated spermatogonia, TAM-treated *Ddx4*^{CreERT2}::*ROSA*^{GRR} testes after 60 days were examined (Figure 13A). One spermatogenesis cycle lasts for 35–40 days [34]. Accordingly, recombinant cells 60 days after TAM injection appear if Cre recombination occurs in undifferentiated spermatogonia. These testes were checked with PNA-lectin, a marker of the acrosome. Only tDsRed-positive sperms were found (Figure 13B). This showed that Cre recombination occurs in undifferentiated spermatogonia in *Ddx4*^{CreERT2} testes.

Immunofluorescence analysis of vimentin, a Sertoli cell marker, showed that the tDsRed signal could not be detected in Sertoli cells (Figure 13B). Taken together, Cre recombination occurred in undifferentiated spermatogonia with 100% efficiency and was restricted to the germ cell lineage in *Ddx4*^{CreERT2} males.

1.2.3 Foxo3-CA cKI mouse evaluation

The mice carrying Foxo3-CA FLEX alleles were considered as *Foxo3*$^{CA\text{-}F/CA\text{-}F}$ mice and used as the control group. The recombined Foxo3-CA FLEX allele was named *Foxo3*$^{CA\text{-}R}$. No abnormalities in ovary morphology were observed in *Foxo3*$^{CA\text{-}F/CA\text{-}F}$ mice compared to wild-type mice (Figure 14A). Similarly, the number of oocytes at all stages was comparable between wild-type and *Foxo3*$^{CA\text{-}F/CA\text{-}F}$ mice (Figure 14B). This result confirmed that oogenesis was normal in *Foxo3*$^{CA\text{-}F/CA\text{-}F}$ mice. To confirm that the flexed alleles can be recombined in oocytes, *Foxo3*$^{CA\text{-}F/+}$::*Gdf9*$^{Cre/+}$ oocytes were fertilized with WT sperm. Genomic PCR showed that 60% of the collected blastocysts were heterozygous *Foxo3*$^{CA\text{-}R/+}$, whereas the remaining blastocysts were wild-type. Moreover, non-recombinant blastocysts were not detected (Figure 14C). The electroporation of *Cre* mRNA into *Foxo3*$^{CA\text{-}F/+}$ embryos was performed, and the recombination rate in the pups at PD1 was determined. Only 13.8% (15/109) of the pups were obtained from electroporated embryos, whereas 59% of non-electroporated pups were delivered. Notably, all pups in both groups were wild-type. This result implies that *Foxo3*$^{CA\text{-}R/+}$ pups die during embryogenesis because the distraction of FOXO3 translocation in the whole body may alter the cell cycle, leading to abnormal embryonic development and lethality.

2. Characterization of oocyte reserve

2.1 Oocyte reserve in congenital model

The influence of oocyte nuclear FOXO3 on oocyte reserve was investigated in a congenital model using *Gdf9*^{Cre} mice, in which recombination started from PD3. The *Foxo3*$^{CA\text{-}R/CA\text{-}R}$::*Gdf9*$^{Cre/+}$ ovaries were collected at 3 months of age. In control mice (*Foxo3*$^{CA\text{-}F/CA\text{-}F}$), FOXO3 was mainly found in the cytoplasm of primary oocytes. The cytoplasmic to nuclear FOXO3 ratio was significantly lower in *Foxo3*$^{CA\text{-}R/CA\text{-}R}$::*Gdf9*$^{Cre/+}$ oocytes than that in the control group. This indicated that FOXO3 was located exclusively in the nucleus of primary oocytes in the congenital model (Figure 15B, C). This result confirmed that mutation in NES successfully prevented FOXO3 from transporting to the oocyte cytoplasm in a congenital model.

The oocyte survival rate in *Foxo3*$^{CA\text{-}R/CA\text{-}R}$::*Gdf9*$^{Cre/+}$ mice was assessed to observe the effects of the accumulation of nuclear FOXO3 on dormant oocyte maintenance and activation. H and E staining showed that there was no distinct difference in ovarian morphology between the control and cKI mice (Figure 15A).

In the ovary, primordial follicles are maintained in the dormant stage. They are then activated and become primary follicles, which are in a growing state. In this study, to classify the primordial or primary follicles, the PCNA signal in the granulosa cell (GC) layer, a marker for proliferation, was utilized. Oocytes surrounded by a single layer of GCs were examined. The follicles with PCNA-negative GCs were primordial follicles (Figure 16A). In contrast, the follicles with PCNA-positive GCs were the primary follicles (Figure 17A). Interestingly, an increase in the number of PCNA-negative GC follicles in cKI mice at 3-months old was observed (Figure 16B), indicating that high

accumulation of nuclear FOXO3 in oocytes supported the survival of the primordial oocyte pool beyond sex maturation.

Next, I examined whether there was any change in the activation of the primordial follicles. Notably, the size of follicles with PCNA-positive GC in *Foxo3*$^{CA\text{-}R/CA\text{-}R}$::*Gdf9*$^{Cre/+}$ mice was significantly smaller than that in the control group (Figure 17B). A comparable number of PCNA-positive GC follicles in cKI mice compared with control mice was observed (Figure 17C). It is suggested that primordial follicles can be activated even when FOXO3 is strictly located in the oocyte nucleus. It is likely that these follicles were partially activated since they could not increase their size as those in the control. Taken together, these results showed that nuclear FOXO3 promoted oocyte reserve before sex maturation occurred in mice.

2.2. Oocyte reserve in acquired model

Previous studies have not clarified how the accumulation of nuclear Foxo3 regulate the maintenance of the primordial follicle pool prior to the aging process. It is unknown whether the accumulation of FOXO3 in the oocyte nucleus occurs after sex maturation to aging can promote the prolongation of the primordial follicle pool. In a congenital model, since nuclear FOXO3 accumulation after Cre recombination from PD3, only the effects of nuclear FOXO3 on oocyte reserve when it accumulates in oocytes before sex maturation can be assessed. Thus, this model is unsuitable for determining whether FOXO3 accumulation in the oocyte nucleus influences the maintenance of oocytes after sex maturation and prior to aging. Therefore, *Ddx4*^{CreERT2} was used to develop the acquired model, in which Cre recombinase activity was mediated by TAM administration. In *Foxo3*$^{CA\text{-}R/CA\text{-}R}$::*Ddx4*$^{CreERT2/+}$ mice, Cre

recombination occurred after TAM was injected at 8-weeks old continuously for 2 weeks. Oocyte development was examined in these mice at the age of 6-months, revealing the function of nuclear FOXO3 in oocyte reserve after sex maturation. A much higher FOXO3 signal intensity was detected to locate solely in the nucleus of cKI primary oocytes compared to that in control oocytes in the acquired model. The cytoplasmic to nuclear FOXO3 ratio in *Foxo3*$^{CA\text{-}R/CA\text{-}R}$::*Ddx4*$^{CreERT2/+}$ oocytes was significantly lower than that in the control group (Figure 18C). This result confirmed that *Foxo3* carrying the mutation in NES in the acquired model stopped FOXO3 from being transported to the cytoplasm of the oocyte.

The oocyte reserve in *Foxo3*$^{CA\text{-}R/CA\text{-}R}$*::Ddx4*$^{CreERT2/+}$ mice was examined to observe the effects of the accumulation of nuclear FOXO3 on primordial follicle maintenance and activation after sex maturation and prior to aging. There was no abnormality in ovarian morphology in *Foxo3*$^{CA\text{-}R/CA\text{-}R}$*::Ddx4*$^{CreERT2/+}$ mice in the acquired model (Figure 18A). Notably, an increase in the number of PCNA-negative GC follicles in *Foxo3*$^{CA\text{-}R/CA\text{-}R}$*::Ddx4*$^{CreERT2/+}$ mice was observed at 6 months of age (Figure 19A, B). This indicated that nuclear FOXO3 could also help prolong the survival of the primordial follicle pool after sex maturation. The size of PCNA-positive GC follicles in *Foxo3*$^{CA\text{-}R/CA\text{-}R}$::*Ddx4*$^{CreERT2/+}$ mice was significantly smaller than that in the control mice (Figure 20A, B), although the number of PCNA-positive GC follicles in *Foxo3*$^{CA\text{-}R/CA\text{-}R}$*::Ddx4*$^{CreERT2/+}$ mice was similar to that in the control mice (Figure 20C). This suggests that the primordial follicles in *Foxo3*$^{CA\text{-}R/CA\text{-}R}$::*Ddx4*$^{CreERT2/+}$ mice were partly activated, even when FOXO3 was accumulated in the oocyte nucleus. Gathering these results, they showed that the accumulation of FOXO3 in the oocyte nucleus encouraged the

maintenance of the primordial follicle pool after sex maturation and prior to the aging process.

DISCUSSION

Oocyte reserve is critical for maintaining the reproductive life span in female mammals. It is known that the PI3K/Akt pathway is a key signaling pathway in the maintenance and activation of the dormant primordial oocyte pool. In particular, FOXO3, a downstream member of this pathway, controls this process. FOXO3 is a transcription factor that regulates the expression of cell cycle related genes. As translocation of FOXO3 from the oocyte nucleus to the cytoplasm and its subsequent degradation in the cytoplasm leads to the activation of dormant oocytes, the role of nuclear FOXO3 when it accumulates in the oocyte nucleus remains controversial. It is unclear whether FOXO3 accumulation causes oocyte death or promotes the survival of dormant oocytes. In this study, I aimed to answer this question. To answer that, I successfully established novel bioresources including Foxo3-CA cKI mice, which express *Foxo3* constitutively in the oocyte nucleus. This novel Foxo3-CA FLEX mouse carries an NES mutation, which can prevent the nuclear-to-cytoplasmic export of FOXO3. This construction is more advantageous than previous models because the phosphorylation sites of FOXO3 are not disrupted and cKIT downstream pathways do not interfere. To induce Cre recombination in my cKI mice, I successfully developed *Gdf9*^{Cre} mice that possess Cre recombination from PD3. This mouse strain showed that recombination occurred mainly in oocytes from the primordial stages. Applying this Cre driver, I created a congenital model (*Foxo3*$^{CA\text{-}R/CA\text{-}R}$*::Gdf9*^{Cre}) to investigate the role of nuclear FOXO3 in oocyte reserve before sex maturation. My results reported a significant increase in the number of dormant primordial oocytes in *Foxo3*$^{CA\text{-}R/CA\text{-}R}$*::Gdf9*^{Cre}. This result showed that nuclear FOXO3 supported the survival rate of primordial oocytes. In previous reports, the effect of nuclear accumulation of FOXO3

on the maintenance or activation of dormant oocytes after sex maturation and prior to aging has not been clarified. To this end, I developed a novel Cre mouse, *Ddx4*^{CreERT2}, in which Cre recombination is controlled by TAM. Using this mouse line, the maintenance of dormant oocytes at 6-months old was assessed. This showed that the population of dormant oocytes significantly increased in the aging stage. Taken together, these results indicate that the accumulation of nuclear FOXO3 can promote the prolongation of dormant oocyte survival in both congenital and acquired models. In *cKit* cKO mice, when *cKit* was deleted in oocytes, oocyte depletion appeared after 8 to 10 weeks of age. In this study, two novel models that caused FOXO3 accumulation in the oocyte nucleus at different time points were established. In the congenital model, FOXO3 accumulated from PD3 and the phenotypes were checked at 3-months old. In contrast, in acquired mice, recombination was induced at 8-weeks old, indicating that FOXO3 began to accumulate after sex maturation. However, both models exhibited similar phenotypes. It is interesting to note that the NES mutation of *Foxo3* did not immediately lead to the observed phenotype in oocyte reserve, but an increase in dormant oocytes could also be reported after sex maturation. Further research is required to identify whether there are any pathways associated with FOXO3 in the maintenance of dormant oocyte pools after sex maturation prior to aging. Together, my study demonstrated that the impact of nuclear FOXO3 accumulation in both developmental phases, before and after sex maturation, did not change.

The models in this study conquered the weaknesses presented in previous research. In particular, *c-Kit* deletion in oocytes disrupted not only the PI3K/Akt pathway but also interfered with other downstream pathways regulating the maintenance and

activation of dormant oocytes. Thus, the pathways regulated by cKIT may contribute to oocyte death. Besides PI3K/Akt, mTOR can also activate primordial oocytes [35]. It was reported that the inhibition of mTORC1 repressed the activation of primordial oocytes, thus maintaining the oocyte pool in mice [36]. Deletion of *rpS6*, downstream of the mTOR pathway, elevated the loss of primordial oocytes through atresia [37]. To check whether cKIT contributes to oocyte survival through this pathway, it is possible to examine oocyte development in a genetically modified model that applies nuclear FOXO3 accumulation in oocytes and knockout of *mTORC1*. If an oocyte's death would be observed in this model, it can help to determine whether cKIT controls oocyte survival through this pathway.

In another study, mutation of threonine 32 and serine 253, 315, 318, 321, and 325 of FOXO3 may interrupt the interaction of FOXO3 and other factors such as protein interaction or DNA binding [19, 38]. FOXO3 is known as a transcription factor that can bind to DNA sequences and regulate gene expression [39]. Thus, the interruption of FOXO3-DNA binding in the oocyte nucleus may alter the expression of target genes involved in oocyte reserve [19]. However, in Foxo3-CA cKI mice, although high accumulation of nuclear *Foxo3* in oocytes was obtained, whether *Foxo3* carrying the NES mutation functioned correctly was not checked. It is important to determine *Foxo3* transcriptional activity in the cKI mice.

One interesting point that was observed in both models was that dormant oocytes were able to wake-up even FOXO3 was highly localized in the oocyte nucleus. This raised the question of why dormant oocytes in cKI mice could be woken up. One possibility is that FOXO3 may be hindered as a transcriptional factor in the nucleus of oocytes to maintain the dormancy of primordial oocytes. FOXO1, a member of the

FOXO family, has been reported to alter DNA binding when FOXO1 is acetylated by CBP, an acetyltransferase [40]. Deacetylation of FOXO1 by SIR2 increases the transcriptional activity of FOXO1 [41]. In *an in vitro* model, it was revealed that deacetylation of FOXO3 by SIR2 enhanced the binding of FOXO3 and DNA [42]. To date, there are no reports on the acetylation of FOXO3 in *an in vivo* system, especially in oocytes. Nevertheless, CBP is found in the cytoplasm of primordial oocytes and is transported to the nucleus of primary oocytes when primordial follicle activation is triggered by PMSG in adult mice [43]. Since FOXO1 and FOXO3 share many similarities in structure and function, based on this evidence, it would be expected that FOXO3 in the oocyte nucleus can be acetylated, leading to the disruption of FOXO3-DNA binding, which affects the expression of possible genes regulating oocyte dormancy and subsequently activates these dormant oocytes.

In conclusion, a novel *Foxo3* constitutively active cKI mouse that was able to induce FOXO3 accumulation in the oocyte nucleus was successfully established. The results suggest that a high amount of nuclear FOXO3 helps to conserve more dormant oocytes in long-term maintenance from a young age to aging. This Foxo3-CA cKI mouse is a useful resource for studying the regulation of ovarian reserve and oocyte development, which are associated with FOXO3.

TABLES

Table 1: PCR primers for genotyping

Mouse	Primer	Sequence	Band size
Foxo3-CA FLEX	Foxo3-CA screening 5out	GCCCCAGGAACTGTGTTCTCC ACTAAT	WT: no band FLEX: 5158bp
	rGpA Rv 68	ATGTCCTTCCGAGTGAGAGAC ACAAAAA	
	rGpA Rv 68	ATGTCCTTCCGAGTGAGAGAC ACAAAAA	WT: no band FLEX: 5181bp
	Foxo3-CA screening 3out	GCTAAAGGAACACTTTGGTAA GGCTCCA	
	Foxo3 CA screening Tg Fw	AGTCTGGGCTTTCAGTGAGC	Tg: 415bp
	Foxo3 CA screening Tg Rv	ATTAATGCAGCTGGCACGAC	
	Cas9 detection Fw	AGTTCAAGCCCATCCTG	Cas9: 959bp
	Cas9 detection Rv	GAAGTTTCTGTTGGCGAAGC	
Gdf9^{Cre}	nlsCre detect primer F	AAAATTTGCCTGCATTACCG	KI 553bp
	nlsCre detect primer R	ATTCTCCCACCGTCAGTACG	
Ddx4^{CreERT2}	*Ddx4*^{CreERT2} screening 5Fw	AGAGAGAGCAAGCTCTTGGA GATTTTCG	WT: no band KI: 3174bp
	Cre Tm68 R2 Rv	CTTTTGCAAGGAATGCGATGA AGTAGAG	
	Cre Tm68 F2 Fw	ACATGAGTAACAAAGGCATGG AGCATCT	WT: no band KI: 3965bp
	Ddx4^{CreERT2} screening 3Rv	TCTGAGGTCCTGTTCCCCTATT GGTACT	

Table 2: List of antibodies

		Primary Antibody	Distributor	Cat.	Dilution solution	Conc.
Immuno-fluorescence staining	Primary Antibody	Rabbit polyclonal anti-MVH	abcam	ab13840	Blocking buffer	1/100
		Mouse monoclonal anti-MVH	abcam	ab27591	Blocking buffer	1/100
		Rabbit monoclonal anti-Foxo3	Abcam	ab70315	Blocking buffer	1/200
		Mouse monoclonal anti-PCNA	Thermo Fisher Scientific	sc-25280	Blocking buffer	1/100
		Guinea pig polyclonal anti-Vimentin	Progen	#GP53	Blocking buffer	1/100
	Secondary Antibody	Goat anti-Mouse IgG (H+L), Superclonal™ Recombinant Secondary Antibody, Alexa Fluor 555	Introvigen	A28180	Blocking buffer	1/100

		Goat anti-Mouse IgG (H+L), Superclonal™ Recombinant Secondary Antibody, Alexa Fluor 647	Introvigen	A28181	Blocking buffer	1/100
		Goat anti-Rabbit IgG (H+L), Superclonal™ Recombinant Secondary Antibody, Alexa Fluor 488	Introvigen	A27034	Blocking buffer	1/100
		Goat anti-Rabbit IgG (H+L), Superclonal™ Recombinant Secondary Antibody, Alexa Fluor 555	Introvigen	A27039	Blocking buffer	1/100
Western blotting	Primary Antibody	Rabbit polyclonal anti-MVH	abcam	13840	Blocking buffer	1/2000

		Anti-mouse monoclonal GAPDH	Proteintech	60004-1-IG	Blocking buffer	1/5000
	Secondary Antibody	Sheep ECL anti-rabbit IgG horseradish peroxidase (HRP)-linked whole antibody	GE Healthcare Life Sciences	NA931V	Blocking buffer	1/30000

Table 3: Primers of RT-PCR

RT-PCR	Primer	Sequence
Ddx4	Ddx4 RT Fw	ACCAAGATCAGGGGACACAG
	Ddx4 RT Rv	GCGACTGGCAGTTATTCCAT
Gapdh	Gapdh RT Fw	ACTCCACTCACGGCAAATTC
	Gapdh RT Rv	CACATTGGGGGTAGGAACAC
Ddx4 (RT-qPCR)	Ddx4 RT-qPCR E3 Fw	GGTGGCTTTGGAAGAGGAAA
	Ddx4 RT-qPCR E5 Rv	TCGCTTGGAAAACCCTCTG
Actb (RT-qPCR)	Actb cDNA primer F	GCTTCTTTGCAGCTCCTTCGT
	Actb cDNA primer R	TCTGACCCATTCCCACCATC

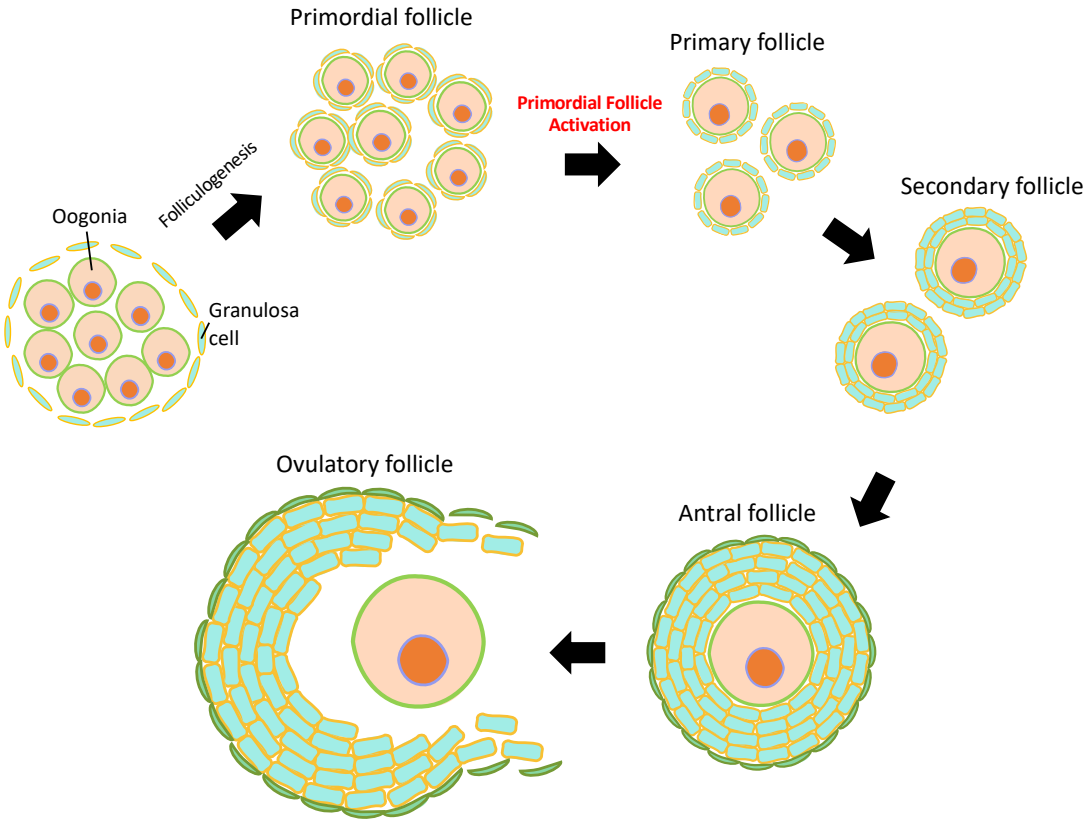

Figure 1: The process of oogenesis.

During embryogenesis, oogonia undergo folliculogenesis, where they are enclosed by flat granulosa cells and become primordial follicles. The primordial follicles remain in the ovary at the dormant stage. After puberty, a small cohort of these follicles is activated and driven into the growth pool to become primary follicles. Subsequently, these primary follicles progress to further developmental stages until they reach ovulation. The remaining primordial follicles keep dormant in the ovary throughout life or are lost with age.

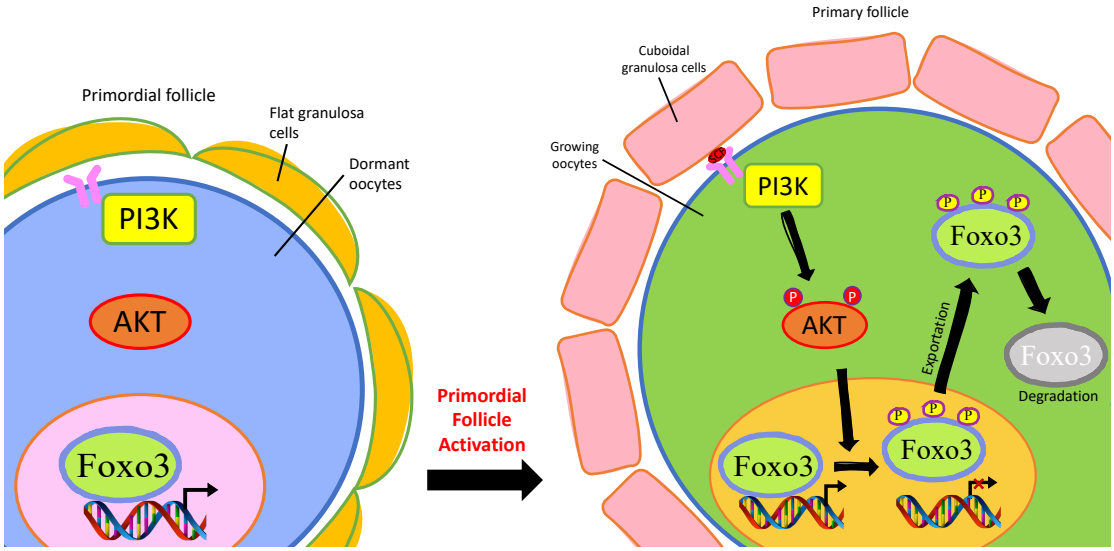

Figure 2: The primordial follicle activation process in oogenesis.

Primordial follicles consist of dormant oocytes that are covered by flat granulosa cells. Many studies have indicated that the PI3K/Akt signaling pathway controls the maintenance and activation of these oocytes. In this pathway, the transcriptional factor FOXO3 is located in the nucleus of dormant oocytes. Under this activation, the PI3K/Akt pathway is activated, which leads to the phosphorylation of FOXO3 and subsequently exports this factor to the oocyte cytoplasm. The nuclear-to-cytoplasmic translocation and loss of FOXO3 result in the activation of oocytes in primordial follicles. The activated follicles are considered primary follicles comprised of growing oocytes surrounded by cuboidal granulosa cells.

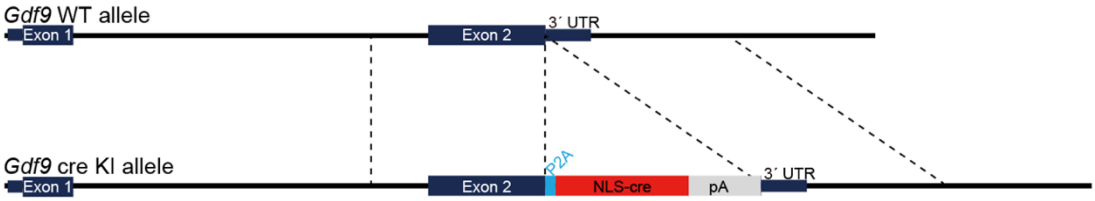

Figure 3: Strategy of *Gdf9*^{Cre} knock-in mice production.

To construct the knock-in allele, P2A connected to the NLS-Cre sequence was knocked-in after the last exon of *Gdf9*.

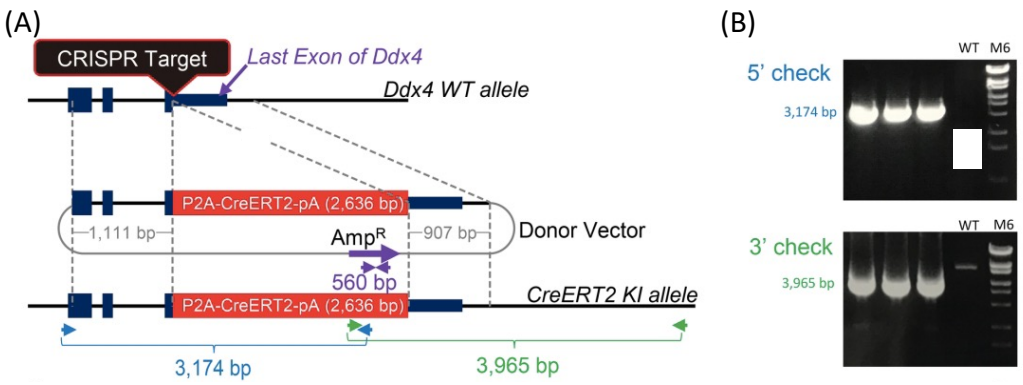

Figure 4: Strategy for *Ddx4*^{CreERT2} knock-in mice production.

(A) Structure of *Ddx4*^{CreERT2} knock-in allele. The P2A-CreERT2-rGpA sequence was integrated before the *Ddx4* stop codon. The 3'-end region of the 5'-homology arm is the final coding sequence of *Ddx4*. The 5' end region of the 3' homology arm is the *Ddx4* stop codon. The blue and green arrows depict primer pairs for detection of the knock-in allele. (B) Representative example of a PCR-positive individual for genotyping.

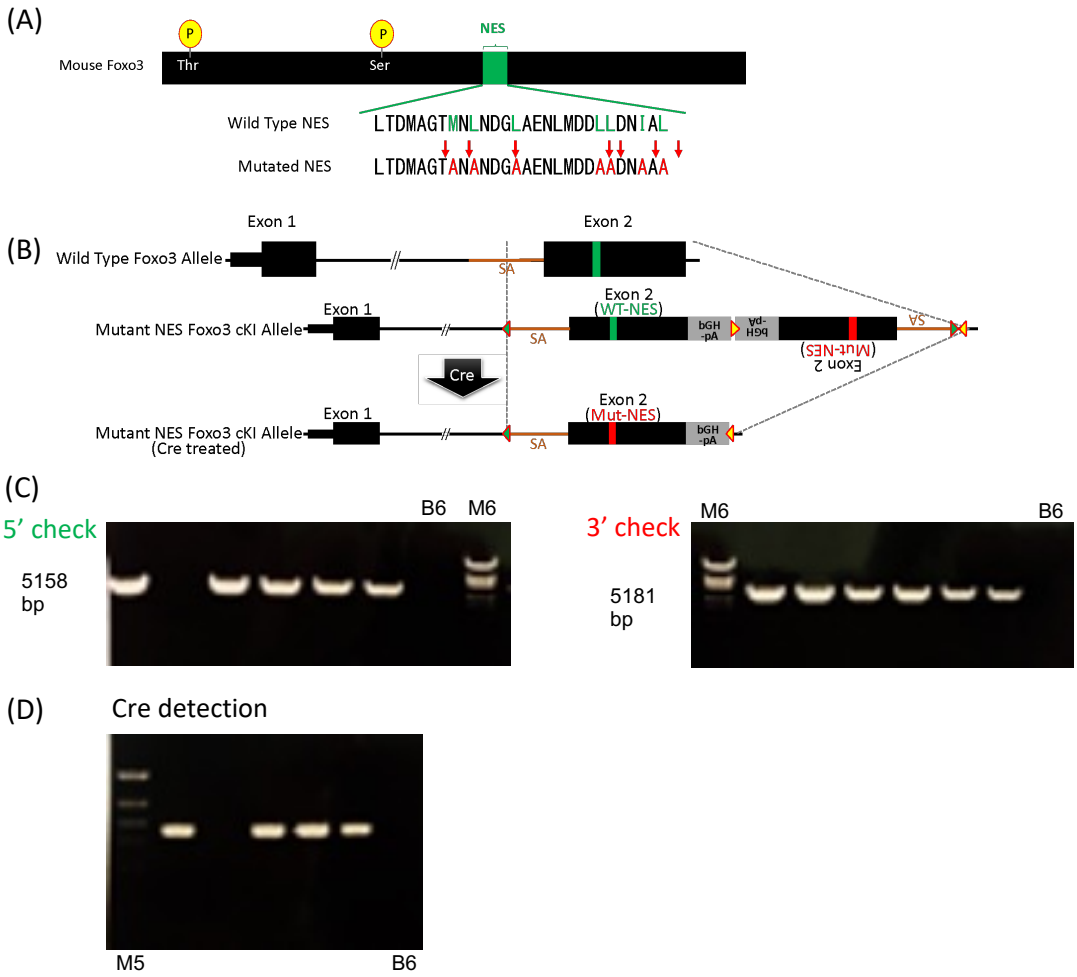

Figure 5: Strategy of Foxo3-CA FLEX mice.

(A) Alanine substitutions in NES in mouse *Foxo3*. (B) Construct of Foxo3-CA FLEX knock-in allele. The mutated NES sequence was integrated between LoxP and Lox2272 in reverse direction. The green arrows indicate the LoxP sites. The yellow arrows depict Lox2272 sites. (C, D) Representative example of a PCR for genotyping. PCR products were amplified using specific primers and genomic DNA from the tail as the template, and the appropriate size was detected.

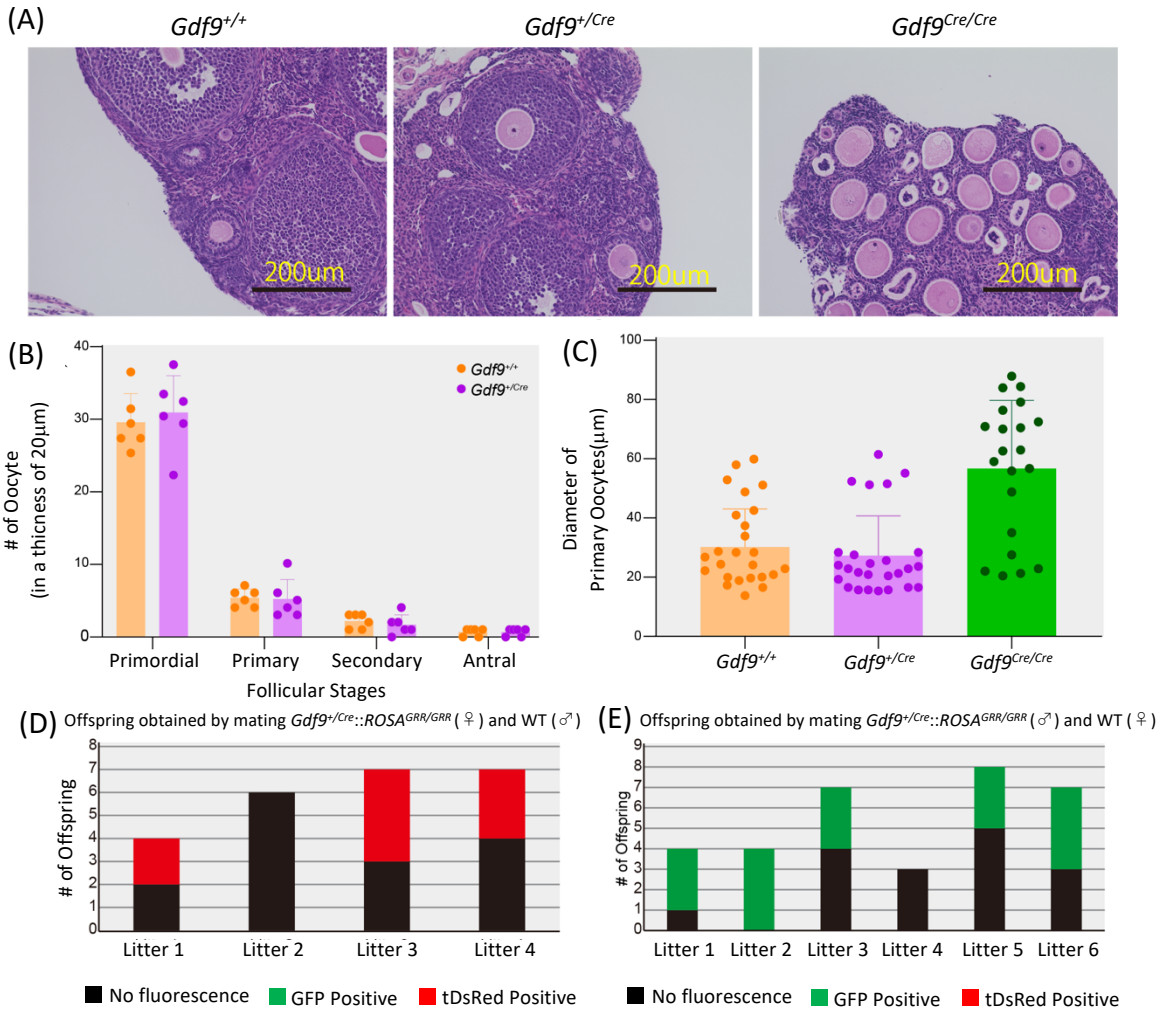

Figure 6: Phenotype of *Gdf9*^{Cre} mice and Cre recombination activity.

(A) The ovarian morphology between wildtype, heterozygous *Gdf9*$^{Cre/+}$, and homozygous *Gdf9*$^{Cre/Cre}$ females was determined via H and E staining. Normal oocyte development was observed in heterozygous *Gdf9*$^{+/Cre}$ mice. In *Gdf9*$^{Cre/Cre}$ mice, primary oocytes were increased in diameter, and there was no presence of secondary oocytes or later stages of oocyte development (Scale bar = 200 µm). (B) The number of oocytes at each stage, including primordial, primary, secondary, and antral oocytes, was recorded. The number of oocytes at each stage was comparable between the wild-types and Gdf9$^{+/Cre}$ mice (n=3, Student's t test, p>0.05). (C) Measurement of primary

oocyte diameter. Homozygous *Gdf9*$^{Cre/Cre}$ mice showed a significant increase in oocyte diameter at the primary stage (n=3, Student's t test, $p<0.05$), confirming that these oocytes failed to proceed further developmental stages beyond primary stage. (D, E) To check the Cre recombination activity in *Gdf9*^{Cre} mice, mice were mated with the reporter R26GRR mice (*ROSA*^{GRR}), which express EGFP and tDsRed before and after Cre recombination, respectively. To check the recombination in oocytes, offspring from *Gdf9*$^{+/Cre}$::*ROSA*$^{GRR/GRR}$ (female) and WT (male) mating were examined. Four litters were checked. No GFP-positive offspring was observed, confirming the recombination occurred in *Gdf9*$^{+/Cre}$ female mice. To check the recombination in sperms, six litters of offspring from *Gdf9*$^{+/Cre}$::*ROSA*$^{GRR/GRR}$ (female) and WT (male) mating were examined. No tDsRed-positive offspring was observed, showing Cre recombination did not happen in *Gdf9*$^{+/Cre}$ male mice.

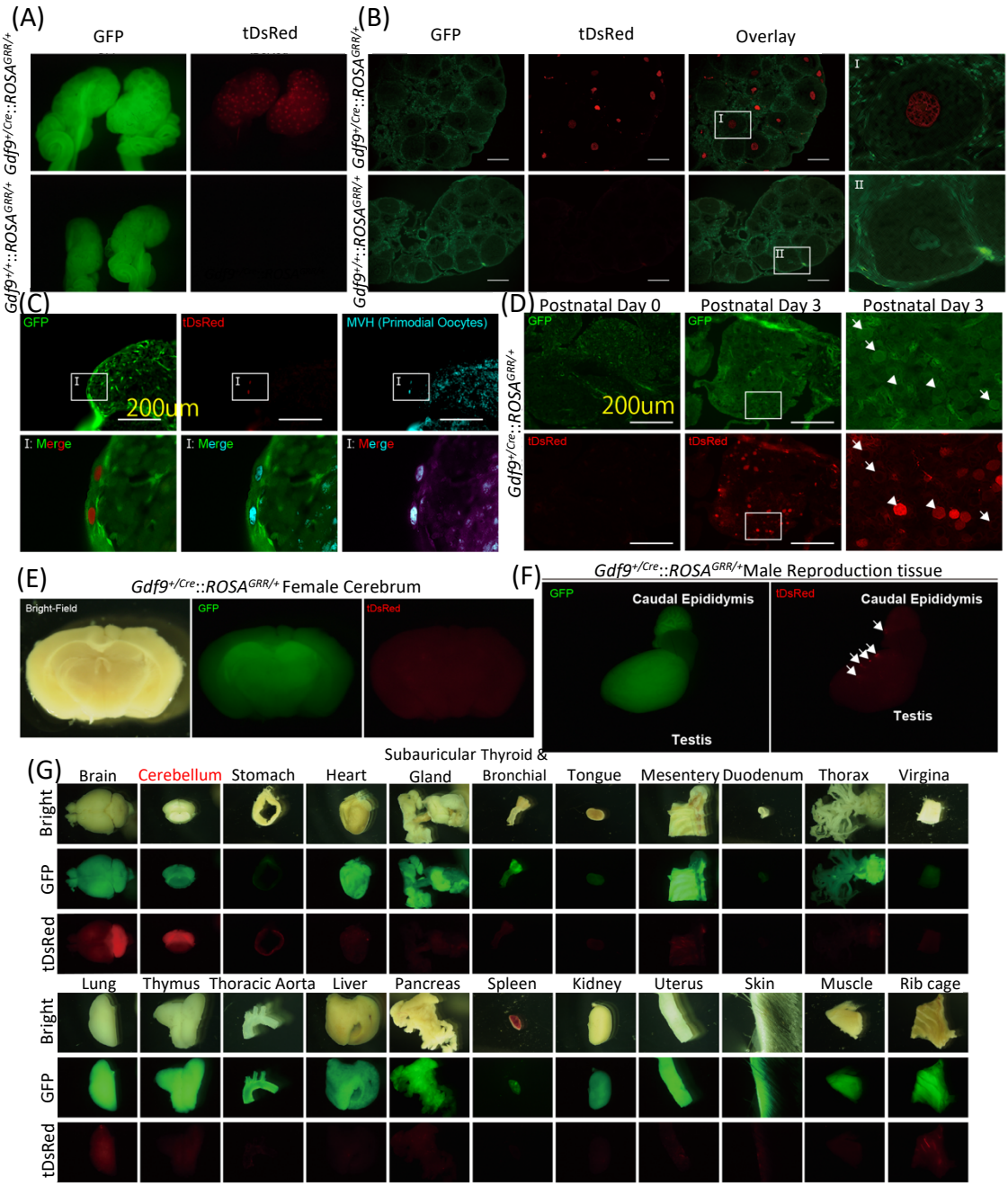

Figure 7: Cre recombination activity in germ cells and other tissues.

(A) tDsRed signal was observed in the ovaries of *Gdf9*$^{+/Cre}$*::ROSA*$^{GRR/+}$ mice. (B) tDsRed signal was present only in oocytes, but not in somatic cells (Scale bar = 50 μm). (C) The Cre recombination occurred from primordial oocytes (Scale bar = 200 μm). (D) The timepoint when the Cre recombination started was determined. At PD0, no tDsRed signal was observed. At PD3, tDsRed-positive oocytes were seen in the *Gdf9*$^{+/Cre}$*::ROSA*$^{GRR/+}$ ovary. Some GFP-positive oocytes were still present in this mice

line. This confirmed that Cre recombination in *Gdf9*^{Cre} mice began from PD3, and the oocytes were completely recombined at adult stage. Arrowheads: Oocytes (Scale bar = 200 μm). (E, F, G) Recombination in other tissues and male reproduction tissues. There was no tDsRed signal observed in other tissues, except from cerebellum and slightly signal in testis. Arrowheads: tDsRed signal detected in testis.

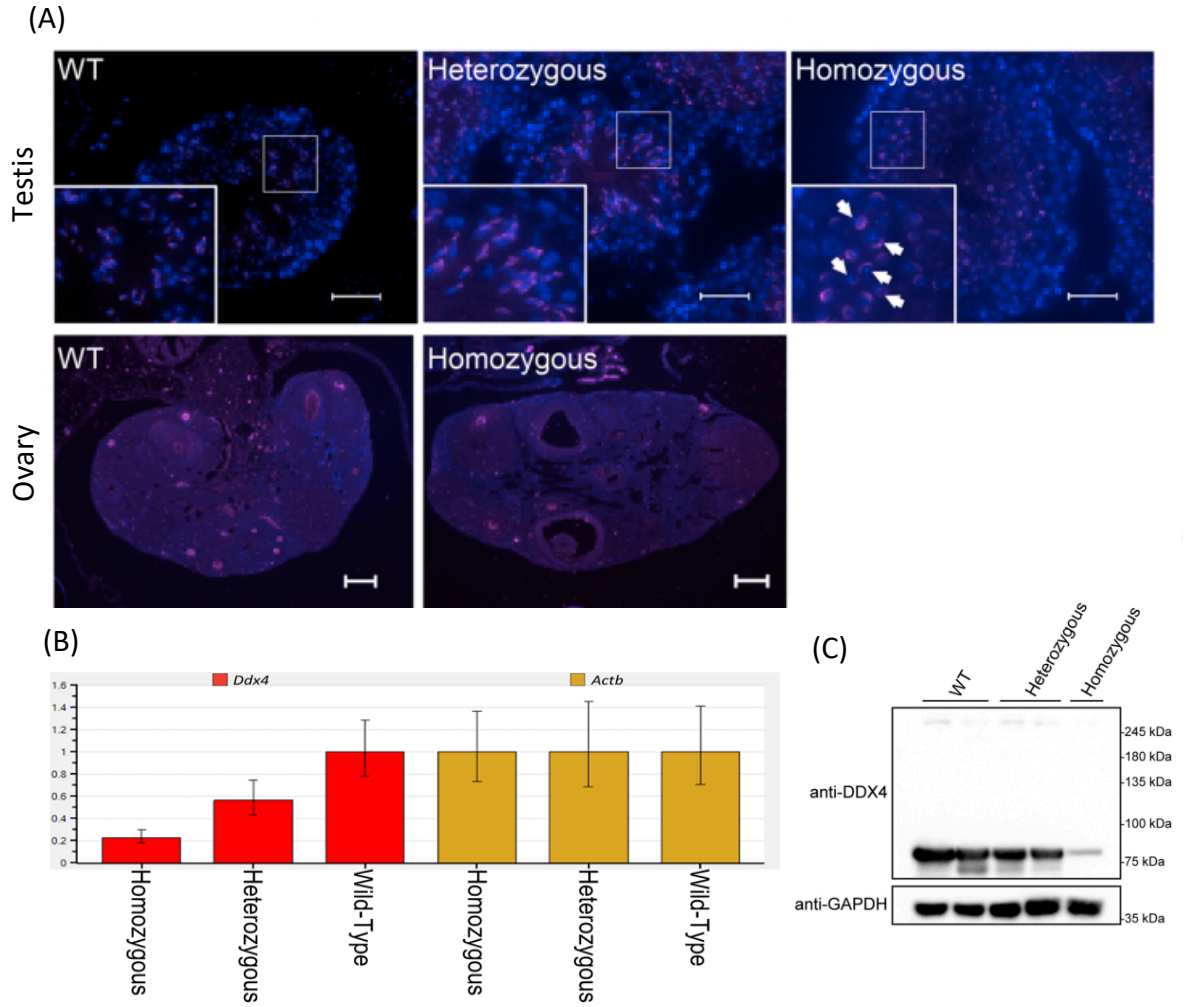

Figure 8: Phenotype of *Ddx4*^{CreERT2} mice and Cre recombination activity.

(A) Germ cell development in heterozygous and homozygous *Ddx4*^{CreERT2} *mice*. In the homozygote testes, round spermatids: PNA-lectin positive cells that had small spherical nucleus (white arrows) (Scale bar = 50 μm). The ovaries from wild-types and homozygous *Ddx4*^{CreERT2} females were stained with DDX4, oocyte markers (Scale bar = 200 μm). DDX4: Purple. PNA-lectin: Purple. DAPI: Blue. (B) Western blotting with heterozygous and homozygous *Ddx4*^{CreERT2} testes. Single DDX4 (76.3 kDa), not fusion protein (153.0 kDa), were detected in the knock-in. Protein levels for DDX4 decreased in the homozygous testis. (C) Quantitative RT-PCR of *Ddx4* in the *Ddx4*^{CreERT2} testes. *Ddx4* mRNA expression in the *Ddx4*^{CreERT2} testes were examined via RT-qPCR. The

expression of *Actb* was used for relative gene expression. *Ddx4* expression in homozygous testis was significantly decreased.

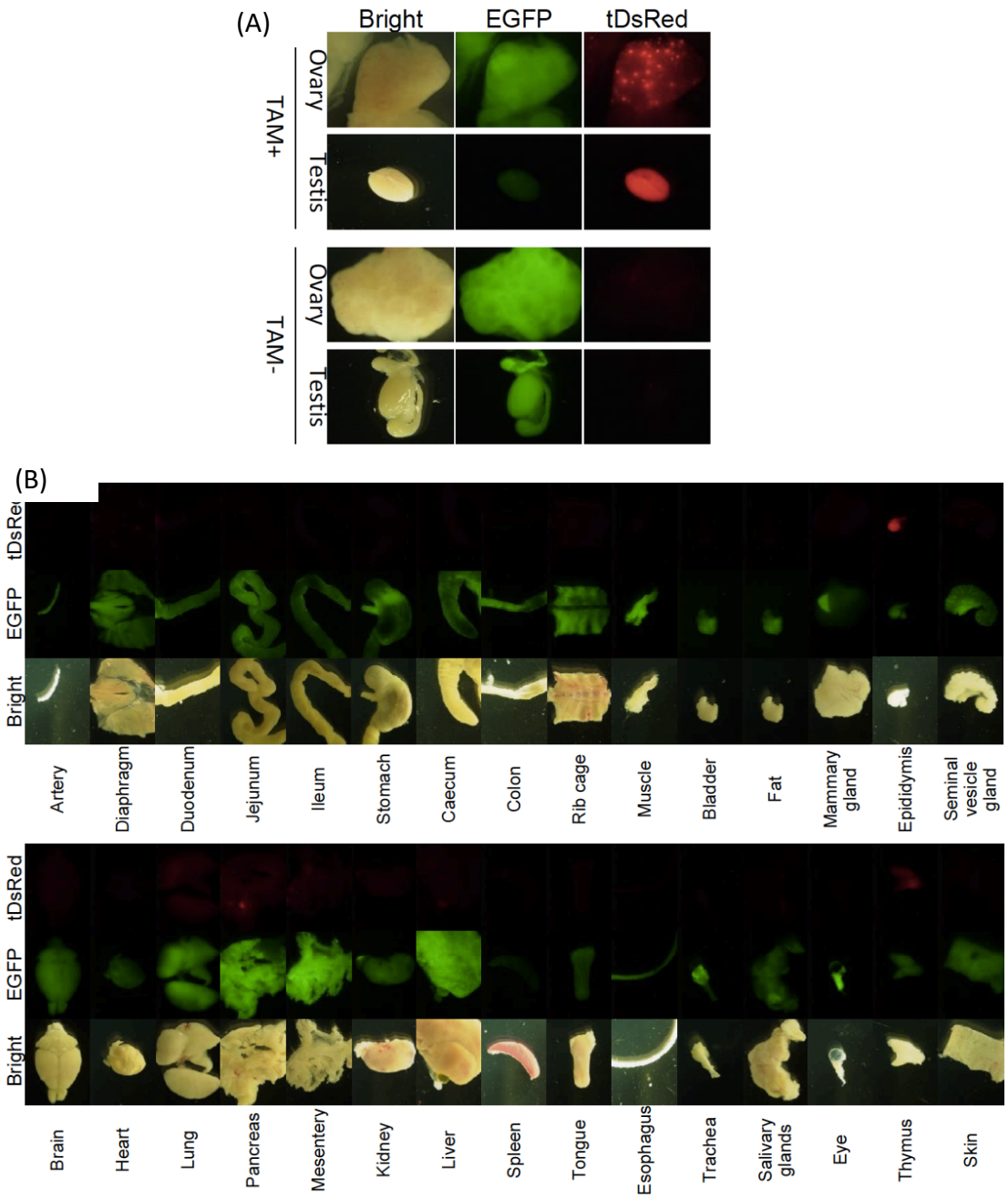

Figure 9: Analysis of Cre recombination in all body parts of *Ddx4*^{CreERT2} mice.

(A) Analysis of Cre recombination in the ovaries and testes of *Ddx4*^{CreERT2}::*ROSA*^{GRR} mice. After TAM injection, EGFP changed to tDsRed signals in both ovaries and testes, whereas only the EGFP signal was found in the controls (without TAM). (B) Systemic analysis of Cre recombination in other tissues. To determine that recombination

occurred solely in the gonads of the knock-in mice, other tissues were collected and observed to detect the tDsRed signal. EGFP: Enhanced green fluorescence.

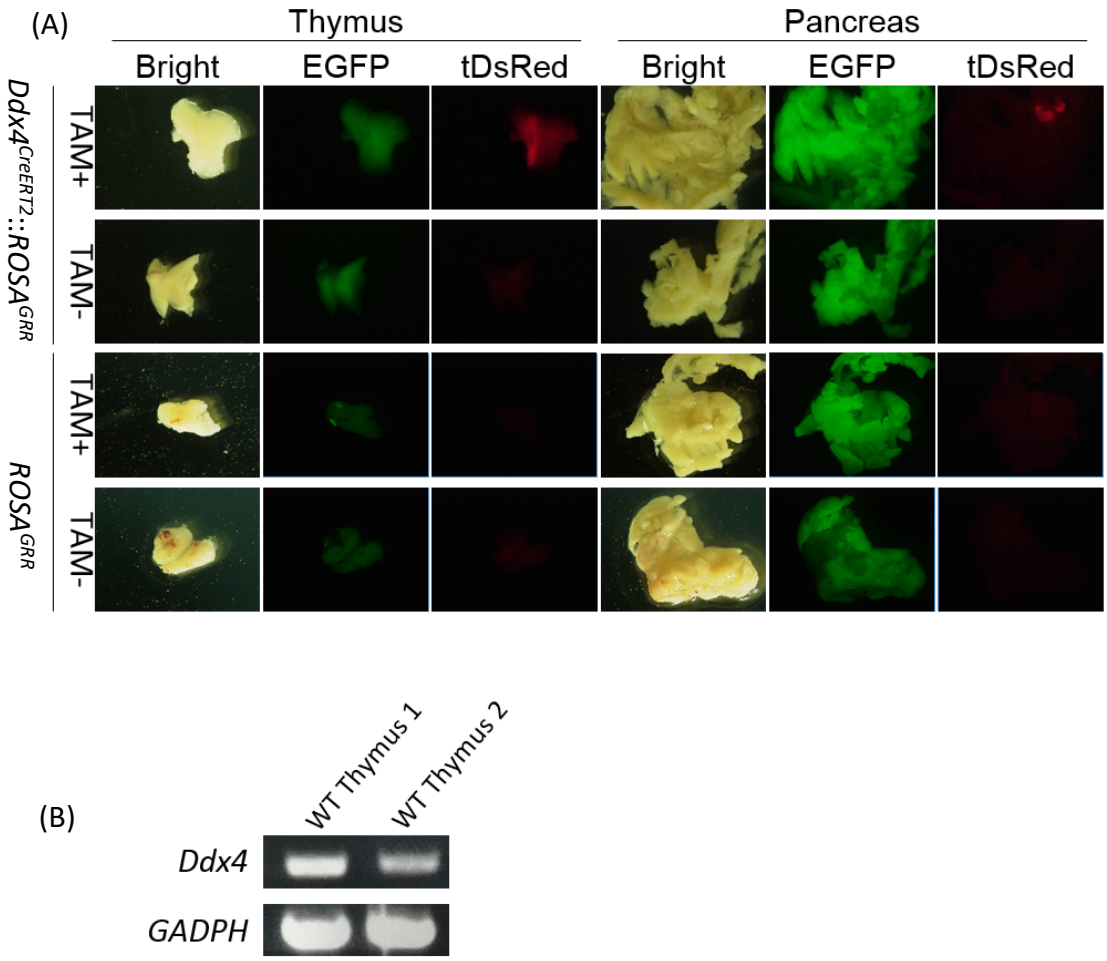

Figure 10: Analysis of Cre recombination in thymus and pancreas.

(A) The tDsRed signals were unexpectedly observed in non-reproductive tissues of *Ddx4*^{CreERT2}::*ROSA*^{GRR} mice. To test whether these were non-specific signals, TAM was injected in *R26GRR*. Only EGFP was detected in the TAM-injected *ROSA*^{GRR} and non-TAM-injected *Ddx4*^{CreERT2}::*ROSA*^{GRR} mice. (B) To determine *Ddx4* expression in the thymus, RT-PCR was performed. *Ddx4* expression in the thymus was confirmed via RT-PCR.

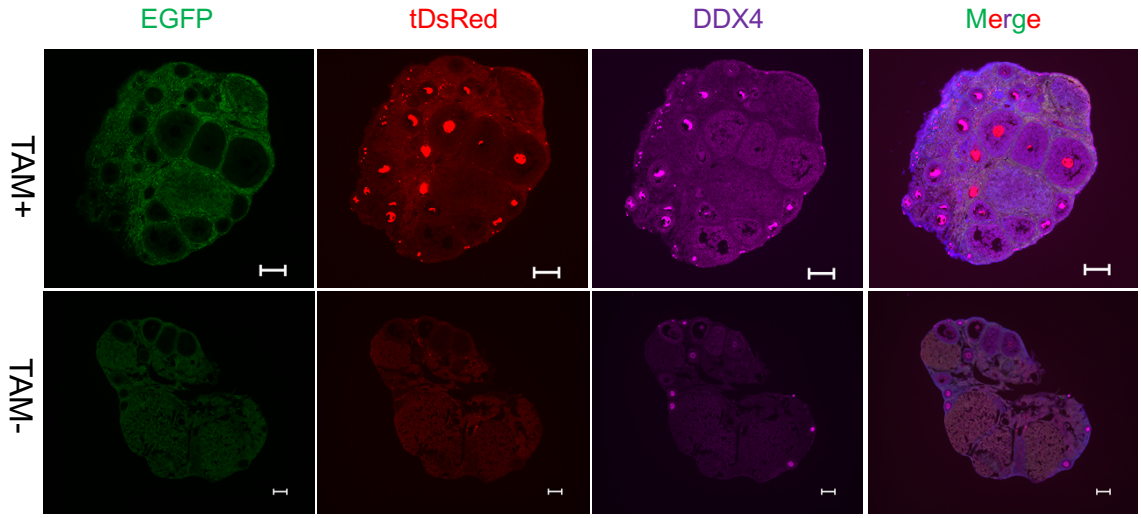

Figure 11: Analysis of Cre recombination efficiency in the oocytes of *Ddx4*^{CreERT2}::*ROSA*^{GRR} mice.

Representative microscopic images of the ovaries in *Ddx4*^{CreERT2}::*ROSA*^{GRR} female mice. To indicate that Cre recombination occurred in the oocytes of *Ddx4*^{CreERT2}::*ROSA*^{GRR} ovaries, immunofluorescent staining of DDX4 was performed (Scale bar = 200 μm). tDsRed-positive oocytes were observed in the TAM-injected *Ddx4*^{CreERT2}::*ROSA*^{GRR} mice. DAPI: Blue.

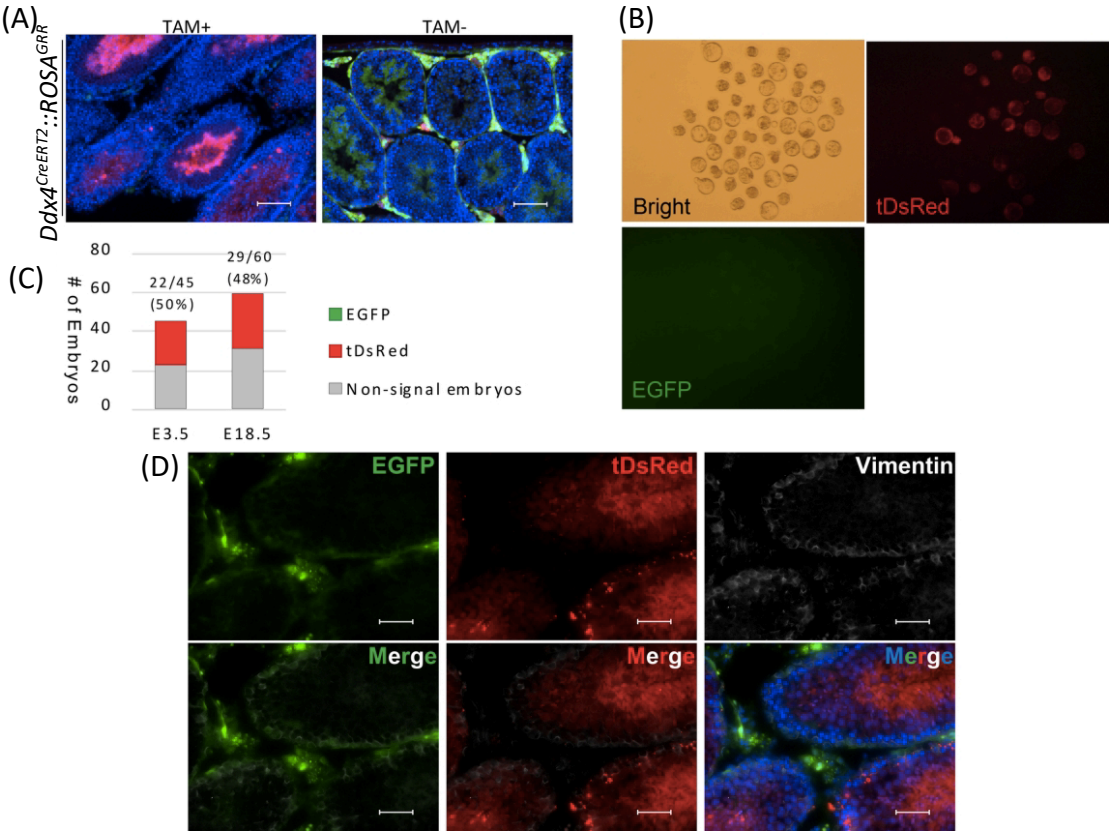

Figure 12: Analysis of Cre recombination efficiency in the testes of *Ddx4*^{CreERT2}*::ROSA*^{GRR} mice.

(A) Immunofluorescence analysis of testes from *Ddx4*^{CreERT2}*::ROSA*^{GRR} male mice. There was no EGFP-positive sperm in the TAM-injected *Ddx4*^{CreERT2}*::ROSA*^{GRR} male mice. DAPI: Blue. (B) Representative images of E3.5 embryos (blastocysts) (Scale bar = 100 μm). (C) Percentage of tDsRed and EGFP embryos at E3.5 and E18.5. (D) To test that Cre recombination occurred in Sertori cells of *B6- Ddx4*^{CreERT2}*::ROSA*^{GRR} mice, testes were stained with Vimentin, the marker for Sertoli cells. No tDsRed signal was observed in Sertoli cells (Scale bar = 50 μm).

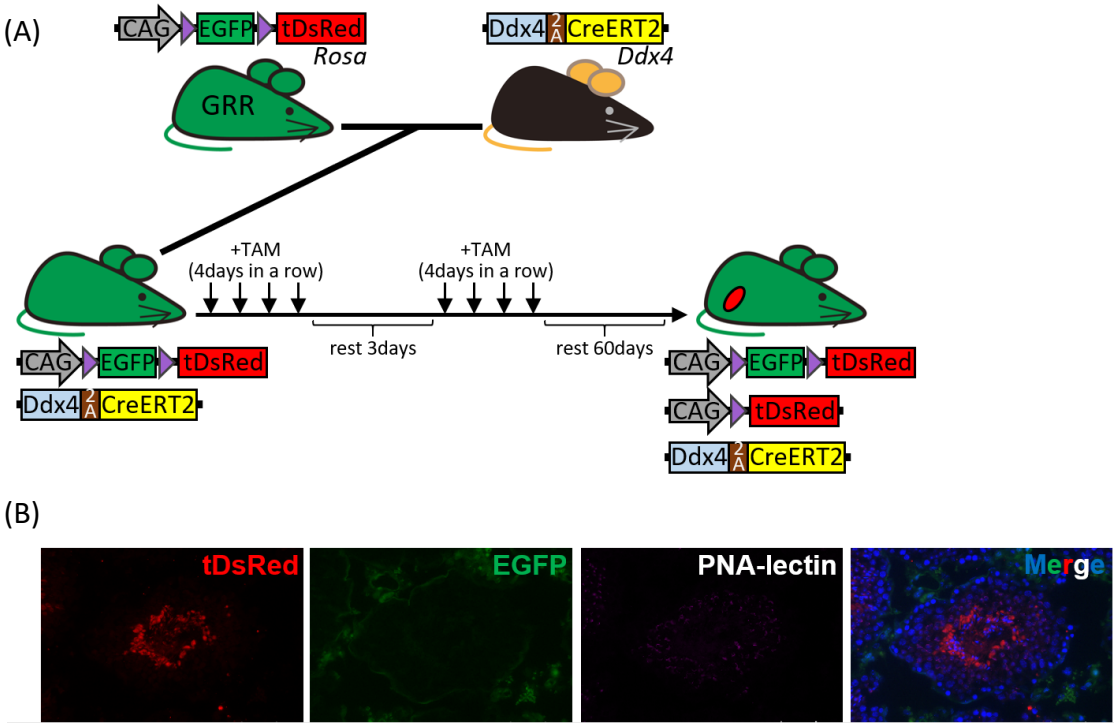

Figure 13: Analysis of Cre recombination in spermatogonia stem cells of *Ddx4*^{CreERT2}*::ROSA*^{GRR} male.

(A) Strategy for mice crossing and TAM injection of B6- *Ddx4*^{CreERT2}*::ROSA*^{GRR} mice. (B) The tDsRed signals were observed in the sperm 60 days after TAM injection. PNA-lectin: Purple. DAPI: Blue.

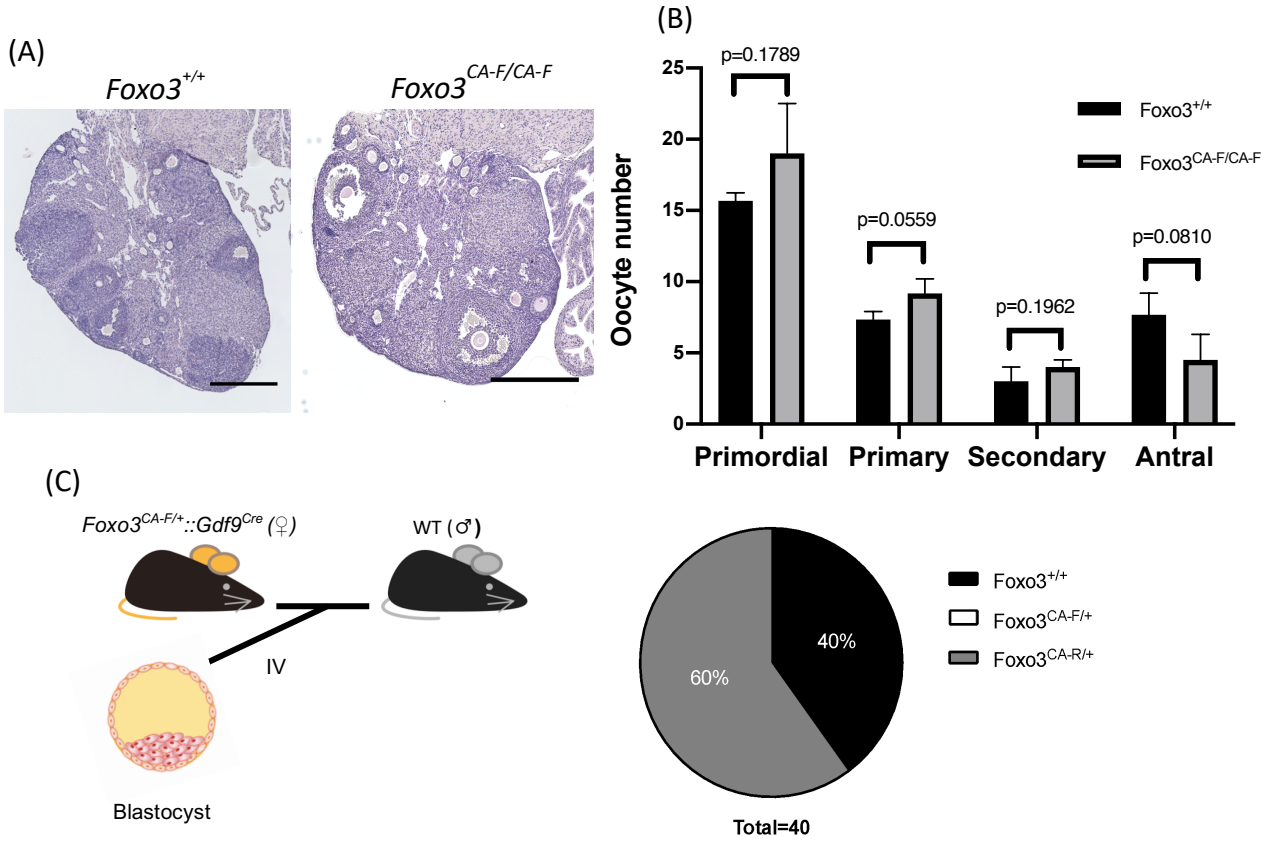

Figure 14: Evaluation of Foxo3-CA FLEX mice.

(A) Morphology of WT and *Foxo3*$^{CA\text{-}F/CA\text{-}F}$ ovaries (Scale bar = 200 µm). (B) The number of oocytes at all developmental stages was calculated. There was no significant difference in the oocyte number between Foxo3-CA FLEX mice and the wildtypes (n=3, Student's t test, p>0.05). (C) IVF between *Foxo3*$^{CA\text{-}F/+}$::*Gdf9*$^{Cre/+}$ oocytes with wild-type sperms to determine the recombination ability of Foxo3-CA KI allele in oocytes. 60% of 40 collected balstocysts were *Foxo3*$^{CA\text{-}R/+}$ and the remaining blastocysts were wild-types (40%).

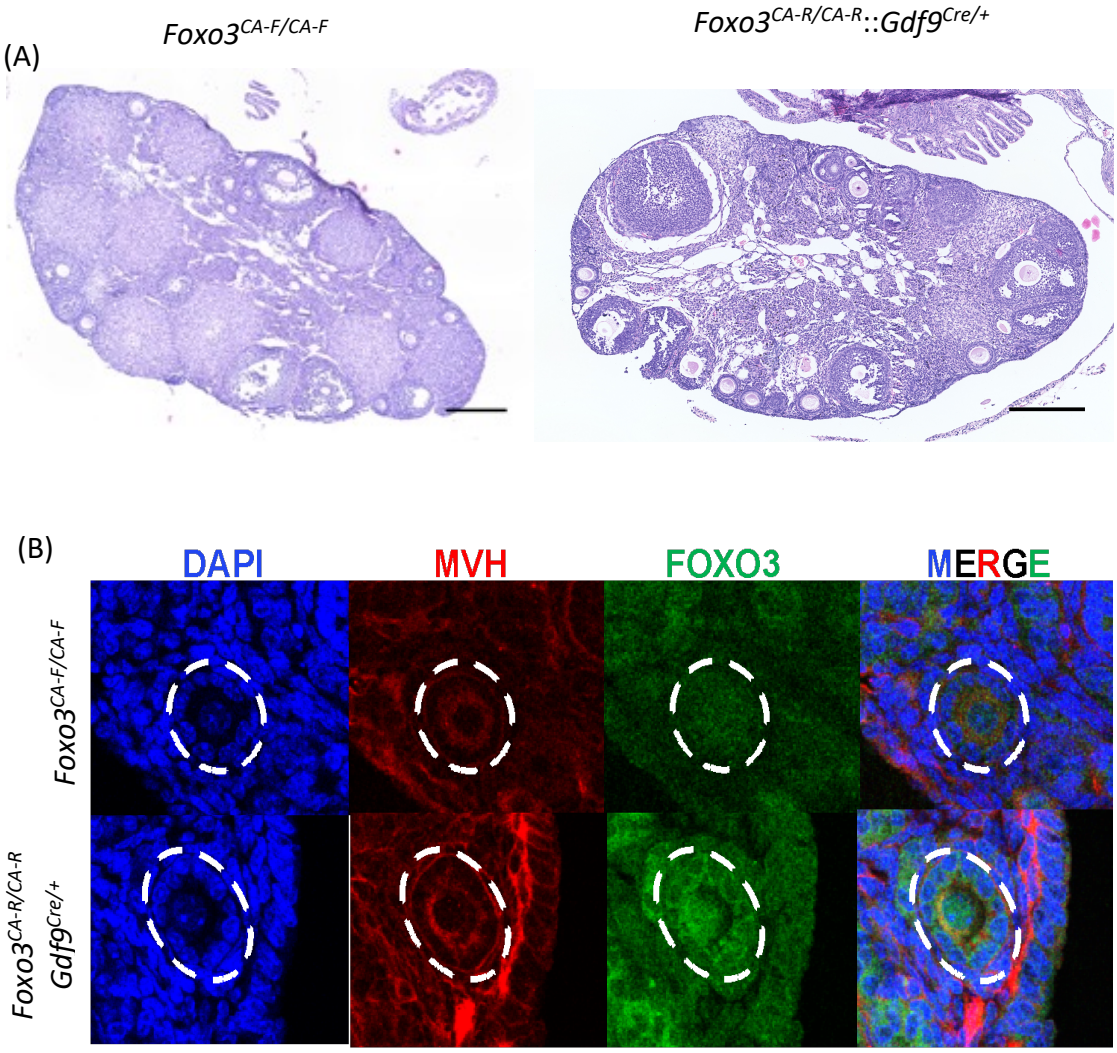
(A)
Foxo3CA-F/CA-F
Foxo3CA-R/CA-R::Gdf9Cre/+
(B)
DAPI
MVH
FOXO3
MERGE
Foxo3CA-F/CA-F
Foxo3CA-R/CA-R Gdf9Cre/+

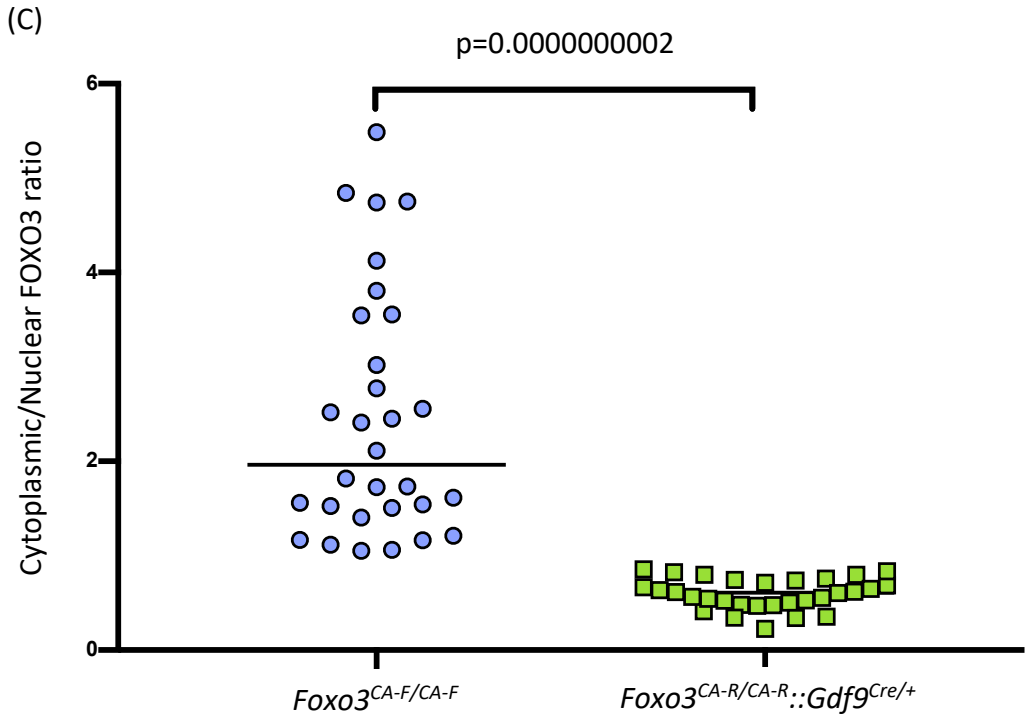

Figure 15: Phenotyping of congenital model.

(A) H and E staining of *Foxo3*$^{CA\text{-}F/CA\text{-}F}$ and *Foxo3*$^{CA\text{-}R/CA\text{-}R}$::*Gdf9*$^{Cre/+}$ ovaries (Scale bar = 200 μm). (B) FOXO3 localization in the primary oocytes of *Foxo3*$^{CA\text{-}R/CA\text{-}R}$::*Gdf9*$^{Cre/+}$ mice at 3 months of age. FOXO3: Green. MVH: Red. DAPI: Blue. (C) The intensity of FOXO3 signal was calculated with ImageJ. Statistical analysis of the ratio of cytoplasmic and nuclear FOXO3 intensity in primary oocytes was performed. There was a significant difference in the cytoplasmic/nuclear ratio of FOXO3 in *Foxo3*$^{CA\text{-}R/CA\text{-}R}$::*Gdf9*$^{Cre/+}$ mice (n=3, Student's t test, $p<0.05$).

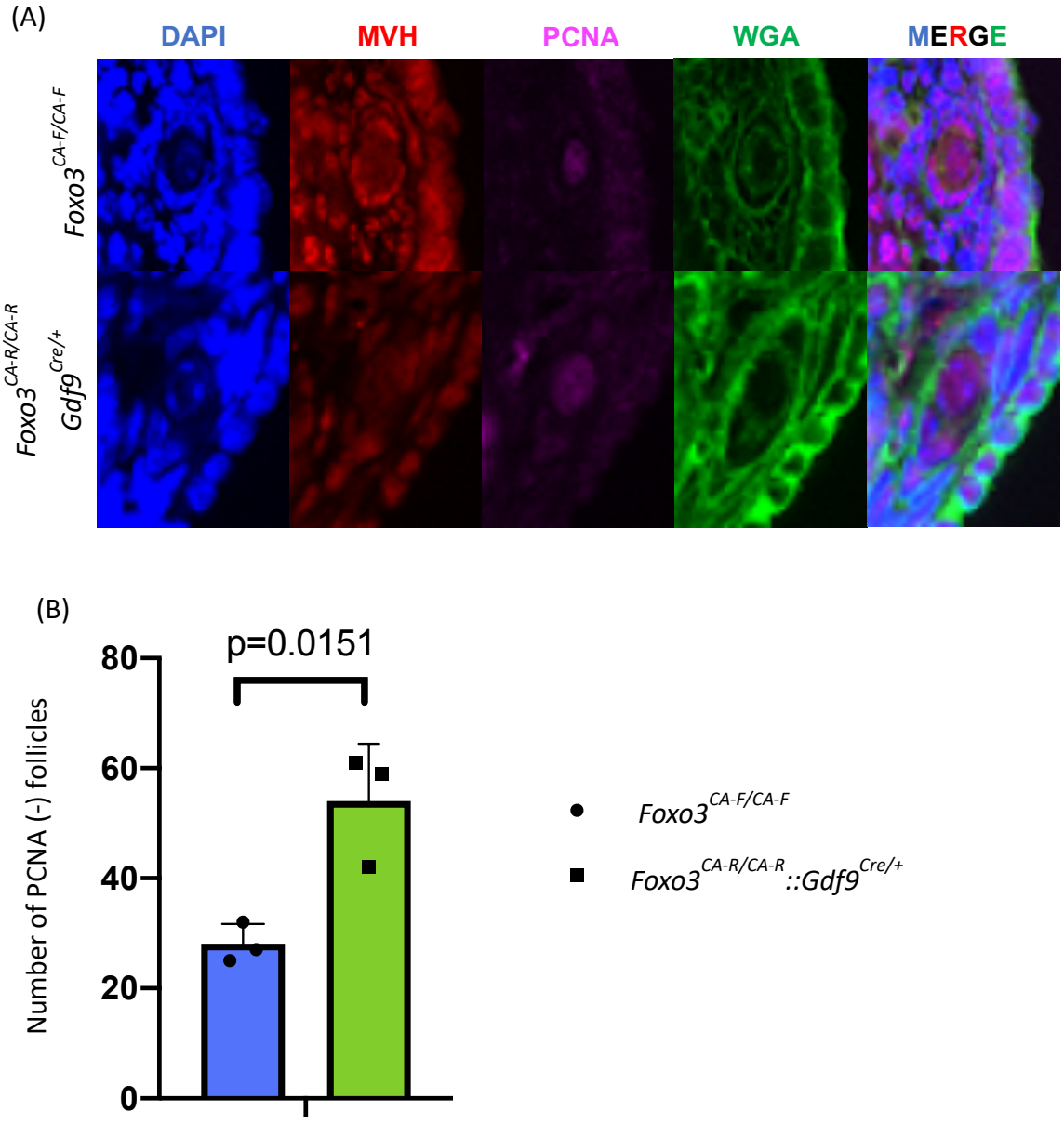

Figure 16: The maintenance of dormant oocytes in congenital model.

(A) Immunofluorescence of PCNA in *Foxo3*$^{CA\text{-}R/CA\text{-}R}$::*Gdf9*$^{Cre/+}$ mice. WGA was used to measure follicle diameter. MVH: Red. PCNA: Purple. WGA: Green. DAPI: Blue. The follicles having PCNA (-)-single layered GC were considered as primordial follicles. (B) The number of PCNA (-) follicles in cKI mice in congenital model was significantly increased (n=3, Student's t test, $p<0.05$).

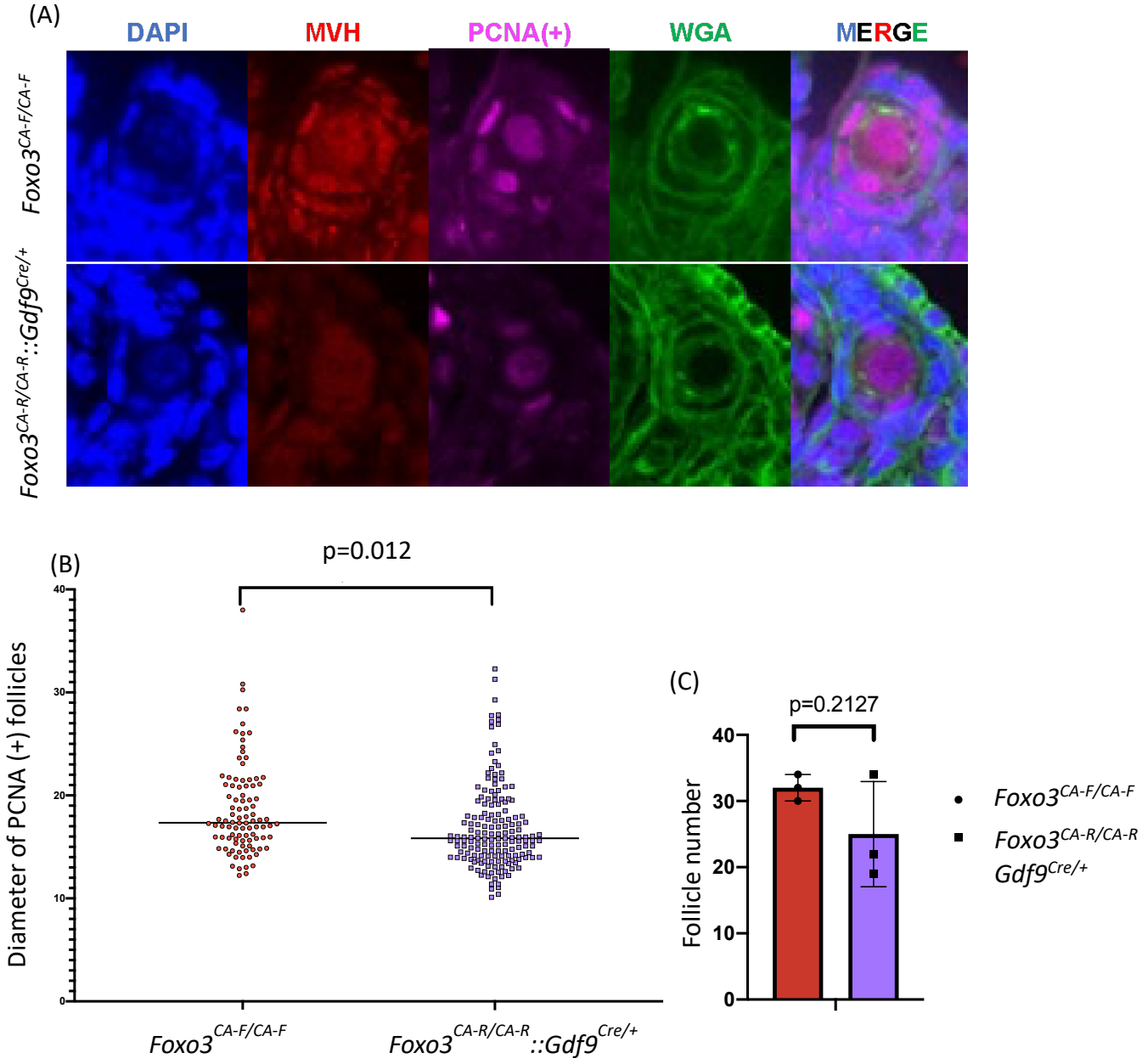

Figure 17: The development of waked-up oocytes in congenital model.

(A) Immunofluorescence of PCNA in *Foxo3*$^{CA\text{-}R/CA\text{-}R}$::*Gdf9*$^{Cre/+}$ mice. MVH: Red. PCNA: Purple. WGA: Green. DAPI: Blue. The follicles with PCNA (+)-single layered GC were considered as primary follicles. (B) The diameter of PCNA (+) follicles in cKI mice was significantly different from that in the control group (n=3, Student's t test, $p<0.05$). (C) The number of PCNA (+) follicles in cKI mice in congenital model was comparable to

that in the control (n=3, Student's t test, $p>0.05$), showing that the dormant oocytes were able to activate.

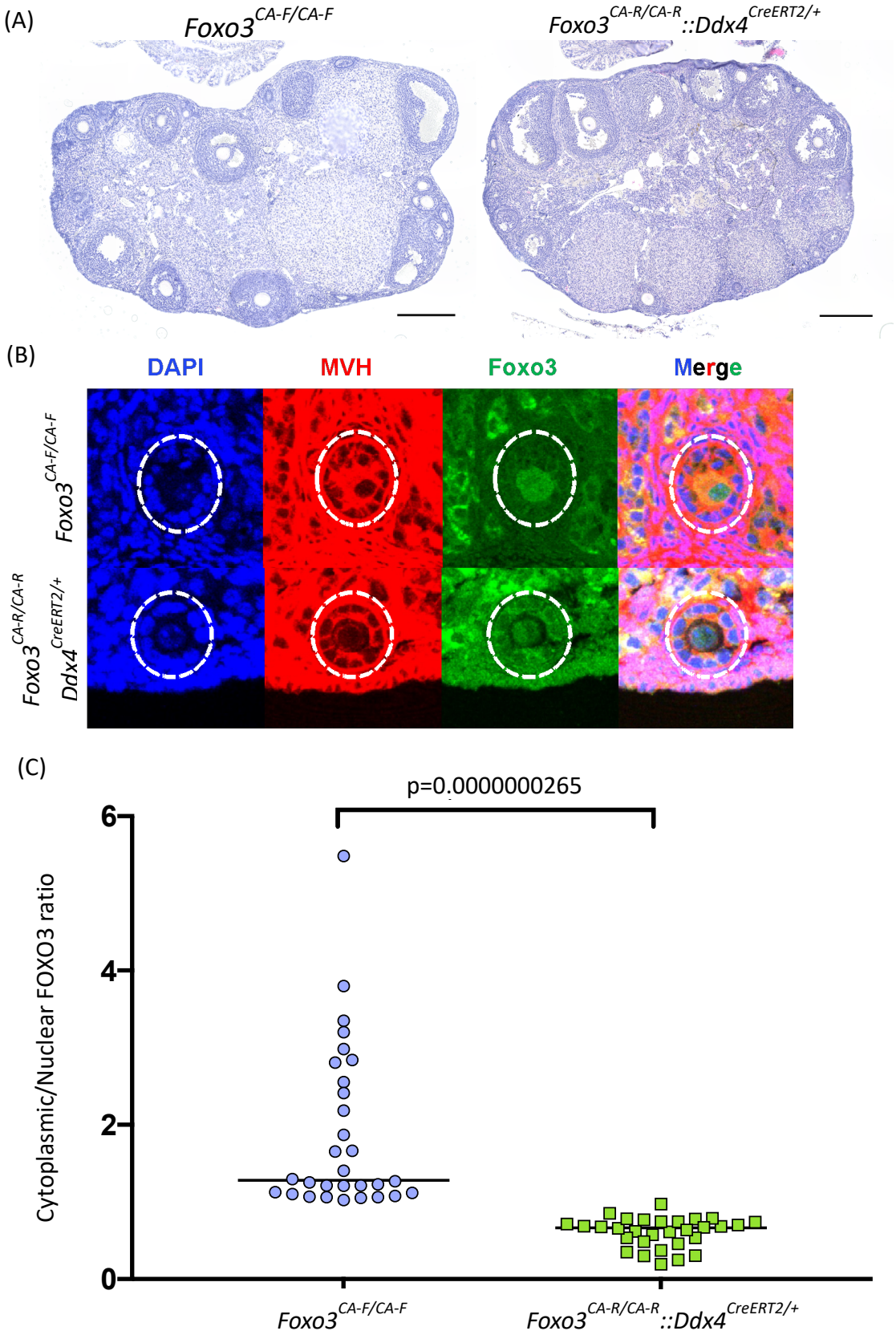
(A)
Foxo3CA-F/CA-F
Foxo3CA-R/CA-R::Ddx4CreERT2/+
(B)
DAPI
MVH
Foxo3
Merge
Foxo3CA-F/CA-F
Foxo3CA-R/CA-R Ddx4CreERT2/+
(C)
p=0.0000000265
Cytoplasmic/Nuclear FOXO3 ratio
6
4
2
0
Foxo3CA-F/CA-F
Foxo3CA-R/CA-R::Ddx4CreERT2/+

Figure 18: Phenotyping of acquired model.

(A) HE staining in *Foxo3*$^{CA\text{-}F/CA\text{-}F}$ and *Foxo3*$^{CA\text{-}R/CA\text{-}R}$::*Ddx4*$^{CreERT2/+}$ mice (Scale bar = 200 μm). (B) FOXO3 localization in the primary oocytes of *Foxo3*$^{CA\text{-}R/CA\text{-}R}$::*Ddx4*$^{CreERT2/+}$ mice at 6-months old. MVH: Red. FOXO3: Green. DAPI: Blue. (C) The intensity of FOXO3 signal was calculated with ImageJ. Statistical analysis of the ratio of cytoplasmic and nuclear FOXO3 intensity in primary oocytes was performed. There was a significant difference in the cytoplasmic/nuclear ratio of FOXO3 in *Foxo3*$^{CA\text{-}R/CA\text{-}R}$::*Ddx4*$^{CreERT2/+}$ mice (n=3, Student's t test, $p<0.05$).

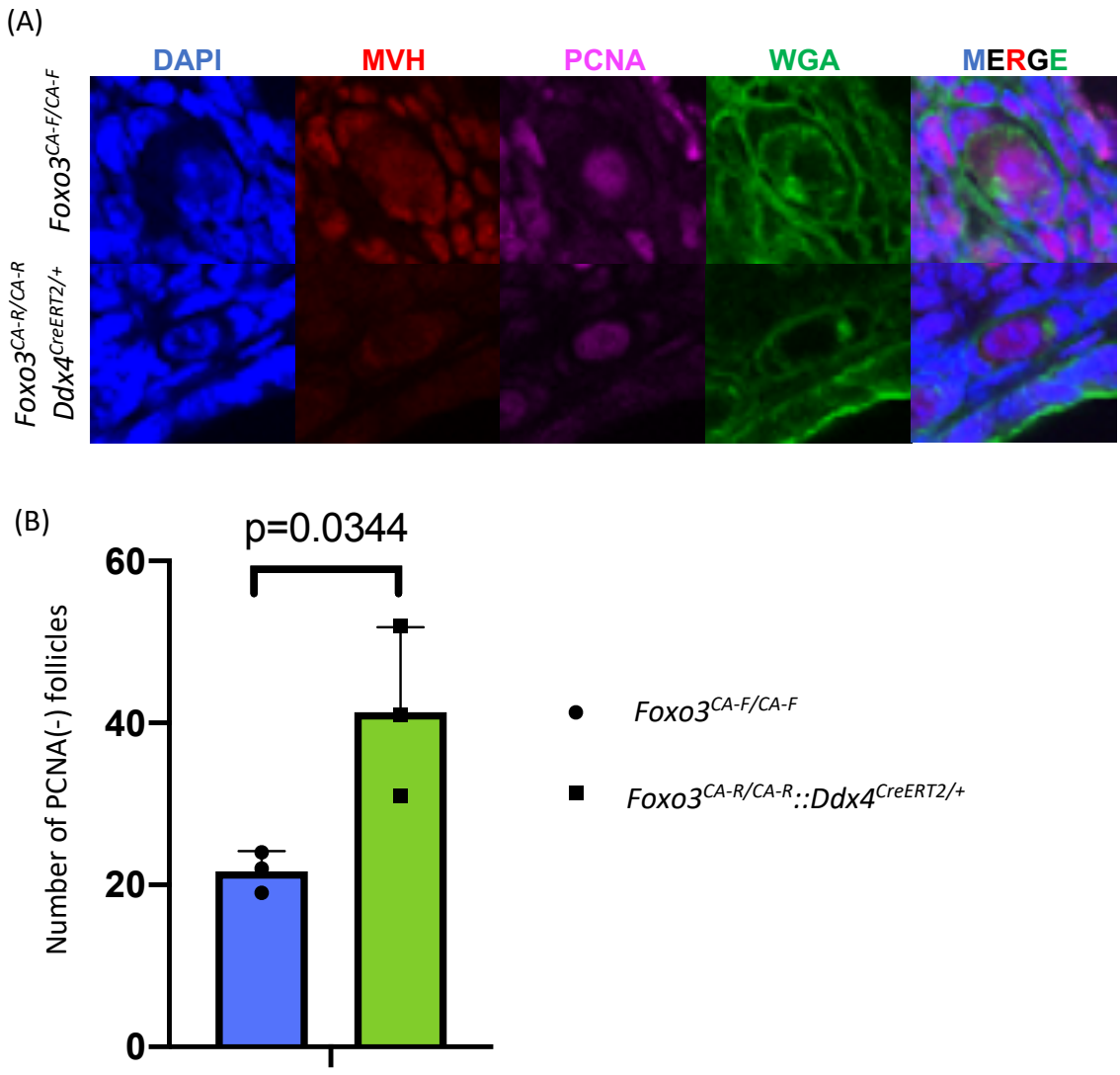

Figure 19: The maintenance of dormant oocytes in acquired model.

(A) Immunofluorescence of PCNA in *Foxo3*$^{CA\text{-}R/CA\text{-}R}$::*Ddx4*$^{CreERT2/+}$ mice. WGA was used to measure follicle diameter. MVH: Red. PCNA: Purple. WGA: Green. DAPI: Blue. The follicles having PCNA (-)-single layered GC were considered as primordial follicles. (B) The number of PCNA (-) follicles in cKI mice in acquired model was significantly increased (n=3, Student's t test, $p<0.05$).

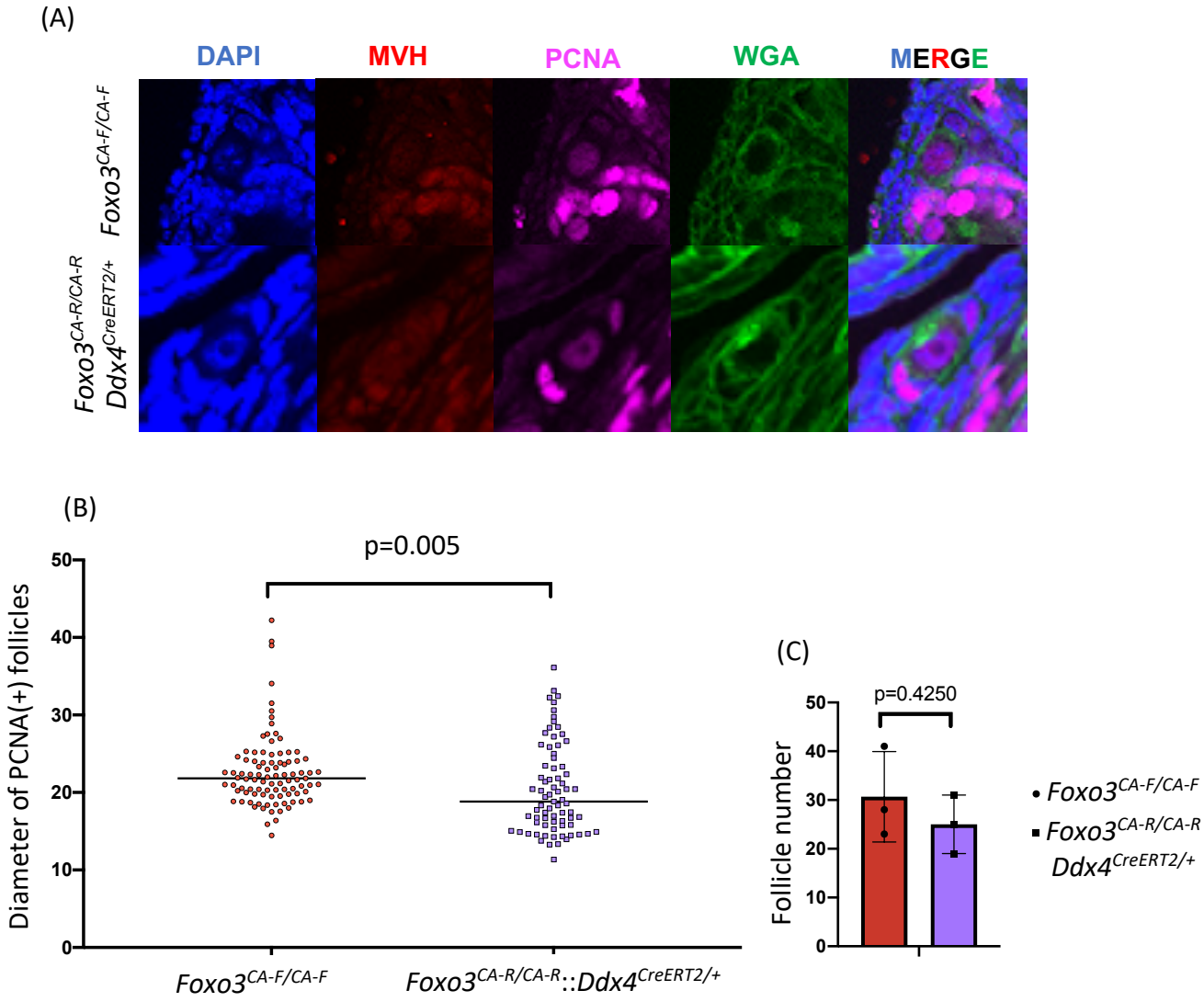

Figure 20: The development of waked-up oocytes in acquired model.

(A) Immunofluorescence of PCNA in *Foxo3*$^{CA\text{-}R/CA\text{-}R}$::*Ddx4*$^{CreERT2/+}$ mice. MVH: Red. PCNA: Purple. WGA: Green. DAPI: Blue. The follicles having PCNA (+) single layered GC were considered as primary follicles. (B) The diameter of PCNA (+) follicles in cKI mice was significantly different to that in the control group (n=3, Student's t test, $p<0.05$). (C) The number of PCNA (+) follicles in cKI mice in acquired model was similar to that in the control group (n=3, Student's t test, $p>0.05$).

ACKNOWLEDGMENTS

I would like to express my great gratitude to Professor Fumihiro Sugiyama for his warm guidance and advice in this research. I would like to express my sincere thanks to my mentor, Associate Professor Seiya Mizuno, for providing knowledge and suggestions during this research, as well as encouraging me and discussion with me to find solutions for the obstacles in this research. Assistant Professor Dinh Thi Huong Tra provided guidance on the experimental techniques. Assistant Professor Kazuya Murata provided advice on experimental analysis and research presentations. In addition, I would like to extend my gratitude to all members of the Laboratory Animal Science of the University of Tsukuba for helping me with many experimental techniques through this research, especially my team members for their support. Last but not least, I would like to express my sincere thanks to my family, seniors, friends, and juniors for supporting me not only in research but also in daily life.

REFERENCES

1. Sarraj, M. A., & Drummond, A. E. (2012). Mammalian foetal ovarian development: consequences for health and disease. Reproduction (Cambridge, England), 143(2), 151–163. https://doi.org/10.1530/REP-11-0247
2. Findlay, J. K., Hutt, K. J., Hickey, M., & Anderson, R. A. (2015). How Is the Number of Primordial Follicles in the Ovarian Reserve Established?. Biology of reproduction, 93(5), 111. https://doi.org/10.1095/biolreprod.115.133652
3. Faddy, M. J., & Gosden, R. G. (1996). A model conforming the decline in follicle numbers to the age of menopause in women. Human reproduction (Oxford, England),11(7),1484–1486. https://doi.org/10.1093/oxfordjournals.humrep.a019422.
4. Zuckerman, Solly. The number of oocytes in the mature ovary. Recent Progress in Hormone Research, 1951, 6: 63-109.
5. McGee, E. A., & Hsueh, A. J. (2000). Initial and cyclic recruitment of ovarian follicles. Endocrine reviews, 21(2), 200–214. https://doi.org/10.1210/edrv.21.2.0394
6. Hornick, J. E., Duncan, F. E., Shea, L. D., & Woodruff, T. K. (2012). Isolated primate primordial follicles require a rigid physical environment to survive and grow in vitro. Human reproduction (Oxford, England), 27(6), 1801–1810. https://doi.org/10.1093/humrep/der468
7. Yan, H., Wen, J., Zhang, T., Zheng, W., He, M., Huang, K., … Wang, C. (2019). Oocyte-derived E-cadherin acts as a multiple functional factor maintaining

the primordial follicle pool in mice. Cell Death & Disease, 10, 160. https://doi.org/10.1038/s41419-018-1208-3.

8. Board, J. A., Redwine, F. O., Moncure, C. W., Frable, W. J., & Taylor, J. R. (1979). Identification of differing etiologies of clinically diagnosed premature menopause. American journal of obstetrics and gynecology, 134(8), 936–944. https://doi.org/10.1016/0002-9378(79)90869-x
9. Russell, P., Bannatyne, P., Shearman, R. P., Fraser, I. S., & Corbett, P. (1982). Premature hypergonadotropic ovarian failure: clinicopathological study of 19 cases. International journal of gynecological pathology: official journal of the International Society of Gynecological Pathologists, 1(2), 185–201. https://doi.org/10.1097/00004347-198202000-00006
10. Zárate, A., Karchmer, S., Gómez, E., & Castelazo-Ayala, L. (1970). Premature menopause. A clinical, histologic, and cytogenetic study. American journal of obstetrics and gynecology, 106(1), 110–114. https://doi.org/10.1016/0002-9378(70)90134-1
11. Starup, J. and Sele, V. (1973), Premature Ovarian Failure. Acta Obstetricia et Gynecologica Scandinavica, 52: 259-268. https://doi.org/10.3109/00016347309158324
12. John, G. B., Gallardo, T. D., Shirley, L. J., & Castrillon, D. H. (2008). Foxo3 is a PI3K-dependent molecular switch controlling the initiation of oocyte growth.

Developmental biology, 321(1), 197–204. https://doi.org/10.1016/j.ydbio.2008.06.017

13. Ren, Y., Suzuki, H., Jagarlamudi, K. et al. Lhx8 regulates primordial follicle activation and postnatal folliculogenesis. BMC Biol 13, 39. https://doi.org/10.1186/s12915-015-0151-3
14. Zhao, Y., Feng, H., Zhang, Y., Zhang, J. V., Wang, X., Liu, D., Wang, T., Li, R., Ng, E., Yeung, W., Rodriguez-Wallberg, K. A., & Liu, K. (2021). Current Understandings of Core Pathways for the Activation of Mammalian Primordial Follicles. Cells, 10(6), 1491. https://doi.org/10.3390/cells10061491
15. Liu, K., Rajareddy, S., Liu, L., Jagarlamudi, K., Boman, K., Selstam, G., & Reddy, P. (2006). Control of mammalian oocyte growth and early follicular development by the oocyte PI3 kinase pathway: new roles for an old timer. Developmental biology, 299(1), 1–11. https://doi.org/10.1016/j.ydbio.2006.07.038
16. John, G. B., Gallardo, T. D., Shirley, L. J., & Castrillon, D. H. (2008). Foxo3 is a PI3K-dependent molecular switch controlling the initiation of oocyte growth. Developmental biology, 321(1), 197–204. https://doi.org/10.1016/j.ydbio.2008.06.017
17. Tzivion G, Dobson M, Ramakrishnan G. (2011). FoxO transcription factors; Regulation by AKT and 14-3-3 proteins. Biochim Biophys Acta, 1813(11):1938-45. https://doi.org/10.1016/j.bbamcr.2011.06.002

18. Wang, X., Hu, S., & Liu, L. (2017). Phosphorylation and acetylation modifications of FOXO3a: Independently or synergistically?. Oncology letters, 13(5), 2867–2872. https://doi.org/10.3892/ol.2017.5851

19. Dobson, M., Ramakrishnan, G., Ma, S., Kaplun, L., Balan, V., Fridman, R., & Tzivion, G. (2011). Bimodal regulation of FoxO3 by AKT and 14-3-3. Biochimica et biophysica acta, 1813(8), 1453–1464. https://doi.org/10.1016/j.bbamcr.2011.05.001

20. Castrillon, D. H., Miao, L., Kollipara, R., Horner, J. W., & DePinho, R. A. (2003). Suppression of ovarian follicle activation in mice by the transcription factor Foxo3a. Science (New York, N.Y.), 301(5630), 215–218. https://doi.org/10.1126/science.1086336

21. Saatcioglu, H. D., Cuevas, I., & Castrillon, D. H. (2016). Control of Oocyte Reawakening by Kit. PLoS genetics, 12(8), e1006215. https://doi.org/10.1371/journal.pgen.1006215

22. Pelosi, E., Omari, S., Michel, M., Ding, J., Amano, T., Forabosco, A., Schlessinger, D., & Ottolenghi, C. (2013). Constitutively active Foxo3 in oocytes preserves ovarian reserve in mice. Nature communications, 4, 1843. https://doi.org/10.1038/ncomms2861

23. Bristol-Gould, S. K., Kreeger, P. K., Selkirk, C. G., Kilen, S. M., Mayo, K. E., Shea, L. D., & Woodruff, T. K. (2006). Fate of the initial follicle pool: empirical and mathematical evidence supporting its sufficiency for adult fertility.

Developmental biology, 298(1), 149–154. https://doi.org/10.1016/j.ydbio.2006.06.023

24. Liew, S. H., Nguyen, Q. N., Strasser, A., Findlay, J. K., & Hutt, K. J. (2017). The ovarian reserve is depleted during puberty in a hormonally driven process dependent on the pro-apoptotic protein BMF. Cell death & disease, 8(8). https://doi.org/10.1038/cddis.2017.361.
25. Hasegawa, Y., Daitoku, Y., Sekiguchi, K., Tanimoto, Y., Mizuno-Iijima, S., Mizuno, S., … Yagami, K. (2013). Novel ROSA26 Cre-reporter knock-in C57BL/6N mice exhibiting green emission before and red emission after Cre-mediated recombination. Experimental Animals, 62, 295–304. https://doi.org/10.1538/expanim.62.295
26. Dong, J., Albertini, D. F., Nishimori, K., Kumar, T. R., Lu, N., & Matzuk, M. M. (1996). Growth differentiation factor-9 is required during early ovarian folliculogenesis. Nature, 383(6600), 531–535. https://doi.org/10.1038/383531a0
27. Rajkovic, A., Pangas, S. A., Ballow, D., Suzumori, N., & Matzuk, M. M. (2004). NOBOX deficiency disrupts early folliculogenesis and oocyte-specific gene expression. Science (New York, N.Y.), 305(5687), 1157–1159. https://doi.org/10.1126/science.1099755
28. Lan, Z. J., Xu, X., & Cooney, A. J. (2004). Differential oocyte-specific expression of Cre recombinase activity in GDF-9-iCre, Zp3cre, and Msx2Cre

transgenic mice. Biology of reproduction, 71(5), 1469–1474. https://doi.org/10.1095/biolreprod.104.031757.

29. Toyooka, Y., Tsunekawa, N., Takahashi, Y., Matsui, Y., Satoh, M., & Noce, T. (2000). Expression and intracellular localization of mouse Vasa homologue protein during germ cell development. Mechanisms of Development, 93, 139–149. https://doi.org/10.1016/s0925-4773(00)00283-5.
30. Brunet, A., Kanai, F., Stehn, J., Xu, J., Sarbassova, D., Frangioni, J. V., Dalal, S. N., DeCaprio, J. A., Greenberg, M. E., & Yaffe, M. B. (2002). 14-3-3 transits to the nucleus and participates in dynamic nucleocytoplasmic transport. The Journal of cell biology, 156(5), 817–828. https://doi.org/10.1083/jcb.200112059.
31. Schnütgen, F., Doerflinger, N., Calléja, C., Wendling, O., Chambon, P., & Ghyselinck, N. B. (2003). A directional strategy for monitoring Cre-mediated recombination at the cellular level in the mouse. Nature biotechnology, 21(5), 562–565. https://doi.org/10.1038/nbt811.
32. Schnütgen, F., De-Zolt, S., Van Sloun, P., Hollatz, M., Floss, T., Hansen, J., Altschmied, J., Seisenberger, C., Ghyselinck, N. B., Ruiz, P., Chambon, P., Wurst, W., & von Melchner, H. (2005). Genomewide production of multipurpose alleles for the functional analysis of the mouse genome. Proceedings of the National Academy of Sciences of the United States of America, 102(20), 7221–7226. https://doi.org/10.1073/pnas.0502273102

33. Atasoy, D., Aponte, Y., Su, H. H., & Sternson, S. M. (2008). A FLEX switch targets Channelrhodopsin-2 to multiple cell types for imaging and long-range circuit mapping. The Journal of neuroscience: the official journal of the Society for Neuroscience, 28(28), 7025–7030. https://doi.org/10.1523/JNEUROSCI.1954-08.2008

34. Tahara, N., Kawakami, H., Zhang, T., Zarkower, D., & Kawakami, Y. (2018). Temporal changes of Sall4 lineage contribution in developing embryos and the contribution of Sall4-lineages to postnatal germ cells in mice. Scientific Reports, 8, 16410. https://doi.org/10.1038/s41598-018-34745-5.

35. Guo, Z., & Yu, Q. (2019). Role of mTOR Signaling in Female Reproduction. Frontiers in endocrinology, 10, 692. https://doi.org/10.3389/fendo.2019.00692

36. Yorino Sato, & Kawamura, K. (2020). Rapamycin treatment maintains developmental potential of oocytes in mice and follicle reserve in human cortical fragments grafted into immune-deficient mice. Molecular and cellular endocrinology, 504, 110694. https://doi.org/10.1016/j.mce.2019.110694

37. Adhikari, D., Zheng, W., Shen, Y., Gorre, N., Hämäläinen, T., Cooney, A. J., Huhtaniemi, I., Lan, Z. J., & Liu, K. (2010). Tsc/mTORC1 signaling in oocytes governs the quiescence and activation of primordial follicles. Human molecular genetics, 19(3), 397–410. https://doi.org/10.1093/hmg/ddp483

38. Boccitto, M., & Kalb, R. G. (2011). Regulation of Foxo-dependent transcription by post-translational modifications. Current drug targets, 12(9), 1303–1310. https://doi.org/10.2174/138945011796150316

39. Hagenbuchner, J., Obsilova, V., Kaserer, T., Kaiser, N., Rass, B., Psenakova, K., Docekal, V., Alblova, M., Kohoutova, K., Schuster, D., Aneichyk, T., Vesely, J., Obexer, P., Obsil, T., & Ausserlechner, M. J. (2019). Modulating FOXO3 transcriptional activity by small, DBD-binding molecules. eLife, 8, e48876. https://doi.org/10.7554/eLife.48876

40. Matsuzaki, H., Daitoku, H., Hatta, M., Aoyama, H., Yoshimochi, K., & Fukamizu, A. (2005). Acetylation of Foxo1 alters its DNA-binding ability and sensitivity to phosphorylation. Proceedings of the National Academy of Sciences of the United States of America, 102(32), 11278–11283. https://doi.org/10.1073/pnas.0502738102

41. Daitoku, H., Hatta, M., Matsuzaki, H., Aratani, S., Ohshima, T., Miyagishi, M., Nakajima, T., & Fukamizu, A. (2004). Silent information regulator 2 potentiates Foxo1-mediated transcription through its deacetylase activity. Proceedings of the National Academy of Sciences of the United States of America, 101(27), 10042–10047. https://doi.org/10.1073/pnas.0400593101

42. Wang, F., Nguyen, M., Qin, F. X., & Tong, Q. (2007). SIRT2 deacetylates FOXO3a in response to oxidative stress and caloric restriction. Aging cell, 6(4), 505–514. https://doi.org/10.1111/j.1474-9726.2007.00304.x

43. Kwok, R. P., Liu, X. T., & Smith, G. D. (2006). Distribution of co-activators CBP and p300 during mouse oocyte and embryo development. Molecular reproduction and development, 73(7), 885–894. https://doi.org/10.1002/mrd.20440

44. Cong, L., Ran, F. A., Cox, D., Lin, S., Barretto, R., Habib, N., Hsu, P. D., Wu, X., Jiang, W., Marraffini, L. A., & Zhang, F. (2013). Multiplex genome engineering using CRISPR/Cas systems. Science (New York, N.Y.), 339(6121), 819–823. https://doi.org/10.1126/science.1231143

45. Osawa, Y., Murata, K., Usui, M., Kuba, Y., Le, H. T., Mikami, N., Nakagawa, T., Daitoku, Y., Kato, K., Shawki, H. H., Ikeda, Y., Kuno, A., Morimoto, K., Tanimoto, Y., Dinh, T., Yagami, K. I., Ema, M., Yoshida, S., Takahashi, S., Mizuno, S., … Sugiyama, F. (2021). EXOC1 plays an integral role in spermatogonia pseudopod elongation and spermatocyte stable syncytium formation in mice. eLife, 10, e59759. https://doi.org/10.7554/eLife.59759.

46. Elvin, J. A., Yan, C., Wang, P., Nishimori, K., & Matzuk, M. M. (1999). Molecular characterization of the follicle defects in the growth differentiation factor 9-deficient ovary. Molecular endocrinology (Baltimore, Md.), 13(6), 1018–1034. https://doi.org/10.1210/mend.13.6.0309

47. Huang, Q., Cheung, A. P., Zhang, Y., Huang, H. F., Auersperg, N., & Leung, P. C. (2009). Effects of growth differentiation factor 9 on cell cycle regulators and ERK42/44 in human granulosa cell proliferation. American journal of

physiology. Endocrinology and metabolism, 296(6), E1344–E1353.

https://doi.org/10.1152/ajpendo.90929.2008